Identification of FAM53C as a suppressive binding protein of a neurodevelopmental disorders-related kinase DYRK1A

Yoshihiko Miyata[1,*] & Eisuke Nishida[1,2]

1 Department of Cell and Developmental Biology, Graduate School of Biostudies, Kyoto University, Kyoto 606-8501, Japan
2 Present address: RIKEN Center for Biosystems Dynamics Research, Kobe 650-0047, Japan
*Corresponding author. E-mail: ymiyata@lif.kyoto-u.ac.jp

Abstract

A protein kinase DYRK1A encoded in human chromosome-21 is the major contributor for multiple symptoms observed in Down syndrome patients. In addition, DYRK1A dysfunction has been associated with various neuronal disorders, including autism spectrum disorder and Alzheimer disease. Here we identified FAM53C as a novel suppressive binding partner of DYRK1A. FAM53C bound to the catalytic kinase domain of DYRK1A, whereas DCAF7/WDR68, the major known DYRK1A-binding protein, binds to its N-terminal domain. The binding of FAM53C inhibited the protein kinase activity of DYRK1A to itself and an exogenous substrate MAPT/Tau. FAM53C did not bind directly to DCAF7/WDR68, whereas DYRK1A tethered FAM53C and DCAF7/WDR68 by binding concurrently to both of them. DYRK1A possesses a nuclear localization signal and accumulates in the nucleus when overexpressed in cells. FAM53C induced cytoplasmic re-localization of DYRK1A and DCAF7/WDR68. FAM53C is thus a binding suppressor of DYRK1A, anchoring it in an inactive state in the cytoplasm. The results explain for the first time why endogenous DYRK1A is distributed in the cytoplasm in the normal brain tissues. FAM53C-dependent regulation of DYRK1A may play a significant role in gene expression modification caused by DYRK1A.

Keywords: DCAF7/Down Syndrome/DYRK1A/FAM53C/Protein Kinase

Character count: 78,245
Word count: 11,681

Introduction

DYRK1A (Dual-specificity tYrosine-phosphorylation Regulated Kinase 1A) is a proline-directed serine/threonine protein kinase belonging to the CMGC family (Becker & Joost, 1999). The amino acid sequence of the catalytic domain of DYRK1A is distantly related to that of MAP kinases (Miyata & Nishida, 1999), implying that DYRK1A may play roles in certain cellular signal transduction systems. DYRK1A phosphorylates pleiotropic substrates both in the nucleus and cytoplasm, and consequently acts as a regulator of the cell cycle, cell quiescence, and cell differentiation (Aranda et al, 2011; Becker & Sippl, 2011; Galceran et al, 2003; Park et al, 2009). DYRK1A is also involved in many other cellular processes such as cytoskeletal organization (Dowjat et al, 2012; Liu et al, 2008; Ori-McKenney et al, 2016; Ryoo et al, 2007; Scales et al, 2009) and DNA damage response (Guard et al, 2019; Menon et al, 2019; Roewenstrunk et al, 2019). Human DYRK1A is encoded in the Down Syndrome Critical Region (DSCR) in chromosome 21 (Galceran et al, 2003; Hämmerle et al, 2003) and higher expression of DYRK1A is responsible for most of the phenotypes including intellectual disability of Down syndrome patients. Model mice with DYRK1A overexpression show phenotypes such as neurodevelopmental delay, motor abnormalities, and cognitive deficits, which are observed in human Down's syndrome patients (Altafaj et al, 2001). A role of DYRK1A has also been suggested in other pathological conditions observed in Down syndrome patients, such as earlier onset of Alzheimer disease (Branca et al, 2017; Kimura et al, 2007; Wegiel et al, 2011), type 2 diabetes (Dirice et al, 2016; Kumar et al, 2021; Rachdi et al, 2014; Shen et al, 2015; Wang et al, 2015; Wegiel et al, 2008), and craniofacial malformation (Blazek et al, 2015; McElyea et al, 2016). In addition, recent studies suggest that DYRK1A is also involved in several other neurodevelopmental disorders including ADHD (Attention Deficit Hyperactivity Disorder) (Tian et al, 2019), ASD (Autism Spectrum Disorder) (De Rubeis et al, 2014; Iossifov et al, 2015; Kim et al, 2017; O'Roak et al, 2012; van Bon et al, 2016; Zhou et al, 2022), and DYRK1A syndrome (also called as MRD7 [Mental Retardation autosomal Dominant 7], see GeneReviews Chapter at https://www.ncbi.nlm.nih.gov/books/NBK333438/) (Bronicki et al, 2015; Courraud et al, 2021; Duchon & Hérault, 2016; Ji et al, 2015). Altogether, it is evident that DYRK1A plays a fundamental role in the process of neurodevelopment and neurofunction. DYRK1A has thus recently emerged in the drug discovery field as one of the most attractive therapeutic target kinases for developing selective inhibitors as new drugs. In contrast to many signaling kinases such as MAP kinases whose activities are regulated by phosphorylation in the activation loop by upstream kinase-kinases, DYRK1A phosphorylates itself in an activation loop tyrosine residue (Tyr321) during the transitional translation process, and this autophosphorylation is essential for the constitutive serine/threonine-specific kinase activity of mature DYRK1A for exogenous substrates (Himpel et al, 2001; Lochhead et al, 2005). The precise molecular mechanism of DYRK1A regulating cellular physiology and human disease conditions, however, remains largely unknown.

Intracellular distribution of DYRK1A is of critical importance and has been a matter of considerable debates. DYRK1A possesses nuclear localization signals (NLS) and thus DYRK1A accumulates inside the nucleus when overexpressed in various cell lines (Álvarez et al, 2003; Becker et al, 1998; Miyata & Nishida, 2011). Many transcription factors, including Nuclear Factor of Activated T-cells (NFAT), FOXO1, and STAT3, are controlled by DYRK1A-dependent phosphorylation in the nucleus (Arron et al, 2006; Bhansali et al, 2021; Gwack et al, 2006). DYRK1A interacts with RNA polymerase II in the nucleus and promotes its hyperphosphorylation in the C-terminal domain repeats through a phase separation mechanism (Di Vona et al, 2015; Lu et al, 2018; Yu et al, 2019). In addition, DYRK1A directly binds to chromatin regulatory regions to control gene expression (Di Vona et al, 2015; Li et al, 2018; Yu et al, 2019). These previous reports indicate that DYRK1A functions in the cell nucleus. On the other hand, endogenous DYRK1A has been often observed in the cytoplasmic and cytoskeletal fractions of cultured cells and natural brains of human and experimental animals (Ferrer et al, 2005; Martí et al, 2003; Wegiel et al, 2004). Taking the constitutive property of DYRK1A activity into account, DYRK1A should be excluded from the nucleus unless absolutely necessary, implying that the intracellular distribution of DYRK1A is strictly regulated by an unknown molecular mechanism.

We and others previously identified DCAF7 (DDB1 and CUL4 Associated Factor 7) [also called as WDR68 (WD Repeat protein 68) or HAN11 (Human homolog of ANthocyanin regulatory gene 11), and we use "DCAF7/WDR68" throughout the text hereafter] as a well-conserved major binding partner for DYRK1A (Mazmanian et al, 2010; Miyata & Nishida, 2011; Morita et al, 2006; Skurat & Dietrich, 2004). Structural analysis indicates that DCAF7/WDR68 forms a seven-propeller ring structure (Miyata et al, 2014) suggesting that DCAF7/WDR68 plays a role in tethering numerous binding partners on its structure as other WD40-repeat proteins. In fact, several proteins, including IRS1, E1A oncoprotein, and RNA polymerase II, have been shown to associate with DYRK1A via DCAF7/WDR68 (Frendo-Cumbo et al, 2022; Glenewinkel et al, 2016; Yu et al, 2019). Likewise, certain proteins may make complexes with DCAF7/WDR68 via DYRK1A. Our earlier phospho-proteomic study obtained more than 250 associating partner candidates for DCAF7/WDR68 (Miyata et al, 2014), which may include uncharacterized DYRK1A-binding proteins.

DYRK1B is the closest relative of DYRK1A with 85% amino acid identities in the catalytic protein kinase domain (Becker et al, 1998), and most of DYRK1A-interacting partners including DCAF7/WDR68 are shared with DYRK1B (Miyata & Nishida, 2011; Varjosalo et al, 2013). On the other hand, Hsp90 (Heat Shock Protein 90) and Cdc37 (Cell Division Cycle protein 37) make a stable complex only with DYRK1B, but not with DYRK1A (Miyata & Nishida, 2021). Identification of additional interacting partners for DYRK1A and DYRK1B is of critical importance to understand the physiological roles of these kinases.

In this study, we have identified FAM53C as a specific binding partner for DYRK1A and DYRK1B. The catalytic kinase domain of DYRK1A was responsible for the FAM53C binding, while DCAF7/WDR68 binds to the N-terminal domain of DYRK1A as previously shown (Glenewinkel et al, 2016; Miyata & Nishida, 2011). Hence, DYRK1A could simultaneously bind to both DCAF7/WDR68 and FAM53C forming a tri-protein complex, demonstrating a tethering function of DYRK1A. The FAM53C binding suppressed the protein kinase activity of DYRK1A. In addition, the binding of FAM53C induced cytoplasmic retention of DYRK1A, and the balance between the levels of DYRK1A and FAM53C determined the intracellular distribution of DYRK1A. These results indicate that FAM53C anchors DYRK1A in the cell cytoplasm in an inactive state. FAM53C may be a key molecule which resolves the long-lasting controversial discrepancy of the intracellular distribution of DYRK1A between overexpressed cell lines and the endogenous setting in our brain.

Results

Identification of FAM53C as a DCAF7/WDR68-DYRK1A interactor

DCAF7/WDR68 is a major binding partner of DYRK1A and DYRK1B (Glenewinkel et al, 2016; Mazmanian et al, 2010; Miyata & Nishida, 2011; Morita et al, 2006; Ritterhoff et al, 2010; Skurat & Dietrich, 2004). By a phospho-proteome analysis, we have previously identified proteins that are physically associated with DCAF7/WDR68, directly or indirectly, along with their phosphorylation sites (Miyata et al, 2014). The most prominent binding partner for DCAF7/WDR68 is a molecular chaperone complex TriC/CCT (Miyata et al, 2014), and some of identified DCAF7/WDR68-associated partners, such as actin and tubulin, may therefore interact with DCAF7/WDR68 indirectly via TRiC/CCT. Similarly, DYRK1A-binding proteins should be possibly included in the DCAF7/WDR68-interactome network. We identified FAM53C, FAMily with sequence similarity 53 member C, in the DCAF7/WDR68-associated phosphoprotein list. The mass analysis identified nine peptides with one phosphoserine each, and they covered 32.1% (126aa in 392aa) of FAM53C in total (Fig 1A). This result indicates that FAM53C is an interacting partner for DCAF7/WDR68.

We then examined the BioPlex (biophysical interactions of ORFeome-based complexes) protein-protein interaction database generated by immunoprecipitation of proteins stably expressed in human cell lines followed by mass spectrometry (Huttlin et al, 2017; Schweppe et al, 2018). The latest update (BioPlex 3.0) of the database incorporates 10,128 (in HEK293T cells) and 5,522 (in HCT116 cells) independent affinity purification–mass spectrometry experiments to create a network of 118,162 interactions among nearly 15,000 proteins (Huttlin et al, 2021). Using DYRK1A as a query (Fig 1B, *upper panels*), both DCAF7/WDR68 (*yellow*) and FAM53C (*orange*) were designated as DYRK1A-interacting partner candidates in HEK293T (*left*) and HCT116 (*right*) cells. Using DCAF7/WDR68 as a query (Fig 1B, *middle panels*), FAM53C (*orange*), as well as DYRK1A (*blue*) and DYRK1B (*magenta*), was listed as an interaction partner in HEK293T (*left*) and HCT116 (*right*) cells. Using FAM53C as a query (Fig 1B, *lower left panel*), the data suggest that all of DYRK1A (*blue*), DYRK1B (*magenta*), and DCAF7/WDR68 (*yellow*) can be FAM53C-binding partners. Finally, both DCAF7/WDR68 (*yellow*) and FAM53C (*orange*) are included in the DYRK1B-interacting network (Fig 1B, *lower right panel*). These protein-protein network analyses convincingly strengthen our result that FAM53C is associated with DCAF7/WDR68 and also with DYRK1A and DYRK1B.

Human FAM53C consists of 392 amino acids and is rich in Ser (16%), Pro (14%), Leu (10%), and Arg (9%), thus, a half of the protein consists of only the four amino acids, making FAM53C a low-complexity sequence protein. Orthologous proteins of FAM53C are encoded in all the mammals examined with high amino acid identities (99% in chimpanzee down to 80% in opossum and 59% in platypus), with lower amino acid identities in lizard/snake (55%), frog (51-52%), turtle/crocodile (43-50%), shark/ray (38%), bonny fish (33-35%), and chicken (33%), but not in cnidarians, nematode, insects, yeast, or plants, suggesting that FAM53C may have vertebrate specific functions. Query for the Phyre2 structural

analysis (http://www.sbg.bio.ic.ac.uk/phyre2/index.cgi) of FAM53C resulted in no obvious similarity with known protein folds. A predicted structure of FAM53C in AlphaFold Protein Structure Database (https://alphafold.com/) shows that the majority of FAM53C structure is highly flexible and thus not rigidly predictable. Prediction by the AlphaFold2 (alphafold2.ipynb: template mode=pdb70, unpaired+paired) indicates that structures of only a limited number of small fragments of FAM53C can be determined with high confidence (Fig 1C). In addition, secondary structure predictions with several algorithms and intrinsically unstructured scores by IUPred2 (https://iupred2a.elte.hu/) both suggest that this protein is composed of coil structures with intrinsically disordered regions throughout the molecule, except short helices in the N- and C-terminal edges and several possible tiny beta-strands (Fig 1C). According to these analyses, FAM53C seems to be a substantially disordered protein with a highly flexible structure. Two related proteins FAM53A and FAM53B are encoded in the human genome and the amino acid identities of FAM53C with FAM53A and FAM53B are 35% and 30%, respectively. FAM53C, as well as FAM53A and FAM53B, has only very limited biochemical and physiological annotations for its function so far.

The human protein atlas database (https://www.proteinatlas.org/ENSG00000120709-FAM53C) indicates that FAM53C is expressed rich in brain and bone marrow, but also expressed in many human tissues with low tissue specificity. The International Mouse Phenotyping Consortium database indicates that FAM53C knock-out mice are viable, showing a phenotype classified as “Decreased exploration in new environment” (https://www.mousephenotype.org/data/genes/MGI:1913556), suggesting that FAM53C may play a role in neurodevelopment and/or neurological function.

Binding of expressed and endogenous FAM53C with DYRK1A and DYRK1B

As described above, we identified FAM53C as a DCAF7/WDR68-interacting protein, and large scale interactome databases suggest that FAM53C may bind to DYRK1A and DYRK1B. We thus examined if FAM53C makes complexes with DYRK1A and DYRK1B by co-immunoprecipitation experiments. DYRK1A and DYRK1B were expressed as 3xFLAG-tagged proteins in mammalian cultured COS7 cells (Fig 2B, *top*) with GFP-FAM53C (Fig 2B, *bottom*) and immunoprecipitated with anti-FLAG antibody (Fig 2A, *top*). The binding of GFP-FAM53C was examined by Western blotting with anti-GFP antibody (Fig 2A, *bottom*). The results indicated that FAM53C bound to and was co-immunoprecipitated with both DYRK1A and DYRK1B.

To examine if endogenous FAM53C binds to DYRK1A and DYRK1B, we made an antibody against FAM53C by immunizing a rabbit with a KLH-conjugated peptide, CQQDFGDLDLNLIEEN, corresponding to amino acids 377-392 (the last 16 amino acids of the C-terminal end) of orangutan FAM53C. The sequence in this region is identical in FAM53C of almost all mammals from opossum to primates. Very few exceptions with one amino acid change are observed in this region of FAM53C of human (Q379R), hylobates (G383R), and echidna/platypus (C377S). Similar sequences are not contained within any other mammalian proteins including the related family proteins FAM53A and

FAM53B. The antiserum was purified on an affinity column of resin conjugated with the antigen peptide. The obtained antibody (Fig 3A, *top right panel*), but not preimmune serum (Fig 3A, *top left panel*), recognized both monkey endogenous (*lane 1)* and exogenously expressed human FAM53C tagged with 3xFLAG (*lane 2*) or with GFP (*lane 3*). COS7 cells were then transfected with 3xFLAG-DYRK1A (Fig 3B, *lanes 3 & 4*) or 3xFLAG-DYRK1B (Fig 3B, *lanes 5 & 6*), and the binding of endogenous FAM53C was examined by co-immunoprecipitation experiments. The binding of endogenous FAM53C was evident in DYRK1A (*lane 4*) and DYRK1B (*lane 6*) immunoprecipitates, only when cells expressed DYRK1A or DYRK1B, and immunoprecipitated with anti-FLAG antibody, but not with control antibody (Fig 3B, *lanes 1-3, & 5*). The antibody against FAM53C recognized several protein bands in the extracts (Fig 3A, *top right panel, lane 1*), and the uppermost band shown by an asterisk corresponds to the FAM53C bound to DYRK1A and DYRKB in Fig 3B, suggesting that this band is full length endogenous FAM53C and a couple of other lower bands might be proteolytic fragments of FAM53C and/or other proteins non-specifically recognized by the antibody. Altogether, these results show that FAM53C binds to both DYRK1A and DYRK1B.

FAM53C binds to the catalytic kinase domain of DYRK1A

The FAM53C-binding domain in DYRK1A was next determined by co-immunoprecipitation experiments. Wild type and deletion mutants of 3xFLAG-tagged DYRK1A were expressed (Fig 4D) with GFP-FAM53C (Fig 4C) and the binding of FAM53C (Fig 4A) to immunoprecipitated DYRK1A (Fig 4B) was determined by Western blotting with anti-GFP antibody. The kinase domain (aa156-479) alone (DYRK1A(K), *lane 3*), but not the N-terminal (aa1-158) (DYRK1A(N), *lane 2*) nor C-terminal (aa481-763) (DYRK1A(C), *lane 4*) domain of DYRK1A, bound to FAM53C. Deletion of the C-terminal domain (DYRK1A(N+K), *lane 5*) or the N-terminal domain (DYRK1A(K+C), *lane 6*) of DYRK1A did not abolish the FAM53C binding. Sufficient levels of GFP-FAM53C expression were observed in all the extracts used for the co-immunoprecipitation assays (Fig 4C). The expression levels (Fig 4D) and the amounts of immunoprecipitated proteins (Fig 4B) of DYRK1A fragments differed with each other, thus it was difficult to accurately estimate the difference of binding levels of DYRK1A domains to FAM53C. These results indicate that the catalytic kinase domain of DYRK1A, but not the N-terminal or C-terminal domain, is responsible for the FAM53C binding. A possible contribution of other parts of DYRK1A outside of the catalytic kinase domain for the FAM53C binding, however, cannot be excluded.

Inhibition of the protein kinase activity of DYRK1A by the FAM53C binding

The effect of the FAM53C binding to the catalytic kinase domain of DYRK1A on its protein kinase activity was then examined. DYRK1A was expressed as a 3xFLAG-tagged protein in cultured COS7 cells with or without FAM53C co-expression and purified with anti-FLAG affinity resin followed by the elution with the 3xFLAG peptide. An equal amount of DYRK1A, alone or in complex with FAM53C, was then incubated in the presence of Mg^{2+}-ATP with purified recombinant MAPT/Tau protein, a

well-established DYRK1A substrate. The levels of DYRK1A-dependent phosphorylation of MAPT/Tau on Thr212 were quantified by Western blotting with a specific anti-pTau Thr212 antibody. As shown in Fig 5A, MAPT/Tau phosphorylation by DYRK1A was much lower when DYRK1A was in complex with FAM53C (*lane 6*) as compared to DYRK1A alone (*lane 5*). The total amount of MAPT/Tau protein was not altered by the incubation for kinase reactions as shown by CBB staining (Fig 5B). The electrophoretic mobilities of DYRK1A were affected when DYRK1A was associated with FAM53C during the kinase reactions. In the absence of expressed FAM53C, a band with a slower mobility (upper band) of DYRK1A was detected (Fig 5C, *lane 5*) while this upper band was not observed when DYRK1A was associated with overexpressed FAM53C (Fig 5C, *lane 6*). The slower mobility (the upper band) of DYRK1A in SDS-PAGE was previously ascribed to phosphorylated species of DYRK1A (Alvarez et al, 2007). Therefore, the slower mobility DYRK1A observed after the kinase reaction (*lane 5*) should be a result of DYRK1A autophosphorylation, and the absence of the phosphorylated DYRK1A band indicates that DYRK1A lost its autophosphorylation activity when bound to FAM53C. Specific binding of FAM53C to DYRK1A was detected by anti-FAM53C Western blotting only when both proteins were concurrently expressed and DYRK1A was isolated with specific affinity resin (Fig 5D, *lane 6*). The binding of endogenous FAM53C to DYRK1A as shown in Fig 3B was not visible at this exposure. MAPT/Tau phosphorylation and the DYRK1A signal were not detected in control conditions (Figs 5A & 5C, *lanes 1-4*). As shown in Figs 5E & 5G, the pTau (Thr212) signal and the DYRK1A mobility up-shift required both Mg^{2+} and ATP (*lane 7-10*), validating that these are ascribed to the Mg^{2+}/ATP-dependent protein phosphorylation reaction. The amounts of MAPT/Tau protein stayed the same (Fig 5F). Taken together, these data indicate that DYRK1A possesses lower protein kinase activity toward both itself and an exogenous substrate when it is associated with FAM53C.

DYRK1A-dependent association of WDR68/DCAF7 with FAM53C

Proteomic as well as co-immunoprecipitation experiments indicate that FAM53C makes a complex both with DYRK1A and DCAF7/WDR68. We next set up an experiment to clarify if FAM53C directly binds to DYRK1A, DCAF7/WDR68, or both. DCAF7/WDR68 was expressed in COS7 cells as an HA-tagged protein with or without 3xFLAG-tagged FAM53C. In addition, GFP-tagged full length or deletion mutants of DYRK1A was concurrently expressed. FAM53C and its associated proteins were immunoprecipitated, and then the binding of DCAF7/WDR68 and DYRK1A was examined by Western blotting. As in the case for the combination of 3xFLAG-DYRK1A and GFP-FAM53C (Figs 2 & 4), 3xFLAG-FAM53C and GFP-DYRK1A were found to be interacted (Fig 6B, *lane 4*). In addition, DCAF7/WDR68 was included in the FAM53C-DYRK1A complex (Fig 6C, *lane 4*). DCAF7/WDR68 could not be co-immunoprecipitated with FAM53C in the absence of DYRK1A (Fig 6C, *lane 3*), suggesting that FAM53C does not bind directly to DCAF7/WDR68. This result is in sharp contrast to the binding of FAM53C to DYRK1A in the absence of exogenously expressed DCAF7/WDR68 (Figs 2-4). Additional co-expression of DYRK1A induced the association between FAM53C and DCAF7/WDR68

(Fig 6C, compare *lanes 3 & 4*), indicating that DYRK1A is required for the binding of DCAF7/WDR68 to FAM53C. Co-expression of DYRK1A-N domain, which binds to DCAF7/WDR68 but not to FAM53C (Fig 6B, *lane 5*), could not induce the association of DCAF7/WDR68 with FAM53C (Fig 6C, *lane* 5). Co-expression of DYRK1A-K domain, which does not bind to DCAF7/WDR68 but binds to FAM53C (Fig 6B, *lane 6*), could not induce the association of DCAF7/WDR68 with FAM53C (Fig 6C, *lane 6*). Contrarily, co-expression of DYRK1A-NK, which possesses both the DCAF7/WDR68-binding N-domain and the FAM53C-binding K-domain, induced association of DCAF7/WDR68 with FAM53C (Fig 6C, *lane 7*) along with DYRK1A-NK (Fig 6B, *lane 7*). Expression levels of FLAG-FAM53C, GFP-DYRKL1A, and HA-DCAF7/WDR68 were shown in Fig 6D-6F. The amounts of immunoprecipitated FAM53C were shown in Fig 6A. A schematic illustration of the expression of three proteins and FAM53C immunocomplexes was shown in Fig 6G. These results indicate that DCAF7/WDR68 is not able to bind directly to FAM53C without DYRK1A, and DCAF7/WDR68 binds to FAM53C in a DYRK1A-dependent manner. In other words, DYRK1A brings DCAF7/WDR68 and FAM53C together with its N-domain and K-domain, respectively.

Intracellular distribution of FAM53C and DYRK1A

To elucidate the intracellular distribution of FAM53C, we expressed GFP-tagged FAM53C in mammalian cultured NIH-3T3 cells. The specific GFP-signal indicated that FAM53C localized in cytoplasmic compartments of cells, and excluded from the nucleus (Fig 7B, *green*). 3xFLAG-DYRK1A when expressed alone localized in the nucleus (Fig 7C, *magenta*), as we and others have shown previously in several cell lines (Álvarez et al, 2003; Becker et al, 1998; Miyata & Nishida, 2011; Miyata & Nishida, 2021). Simultaneous expression of FAM53C with DYRK1A resulted in cytoplasmic re-distribution of DYRK1A (Fig 7D, *magenta*) and DYRK1A co-localization with FAM53C (Figs 7D & 7E), suggesting that FAM53C functions as a cytoplasmic anchoring protein for DYRK1A. The same conclusion was obtained when we exchanged the tags for FAM53C and DYRK1A as follows. 3xFLAG-FAM53C localized in the cytoplasm and excluded from the nucleus (Fig 7F, *magenta*), while GFP-DYRK1A accumulated in the nucleus when expressed alone (Fig 7G, *green*). Co-expression of FAM53C with DYRK1A induced cytoplasmic retention of DYRK1A (Fig 7H), resulting in co-localization of DYRK1A with FAM53C in the cytoplasm (Figs 7H & 7I), again indicating the cytoplasmic anchoring function of FAM53C toward DYRK1A. In same microscopic fields, we often observed that DYRK1A was excluded from the nucleus of cells (*green*) where FAM53C expression levels (*magenta*) were high (Figs 7J & 7K, *arrows*). On the other hand, DYRK1A remained in the nucleus of cells where only low or no FAM53C was expressed (Figs 7J & 7K, *arrow heads*). This relationship between FAM53C expression levels and DYRK1A localization shows that FAM53C regulates intracellular distribution of DYRK1A. Taken together, these results indicate that FAM53C binding suppresses nuclear accumulation of DYRK1A in cells and anchors DYRK1A in the cytoplasm.

Tethering function of DYRK1A

We have previously reported that DYRK1A binds to DCAF7/WDR68 and induces its nuclear accumulation (Miyata & Nishida, 2011). We then examined if FAM53C modifies the DYRK1A-induced nuclear localization of DCAF7/WDR68. When expressed alone, GFP-DCAF7/WDR68 localized both in the cytoplasm and nucleus (Fig 8A, *green*). Co-expression of HA-DYRK1A which accumulated in the nucleus (Fig 8B, *magenta*) induced nuclear co-localization of DCAF7/WDR68 with DYRK1A (Fig 8B, *green*). Additional expression of 3xFLAG-FAM53C resulted in cytoplasmic re-localization of DYRK1A (Fig 8D, *magenta*) as observed in Fig 7, and therefore, DYRK1A lost its ability to induce nuclear re-localization of DCAF7/WDR68 (Fig 8D, *green*). Expression of 3xFLAG-FAM53C (Fig 8C, *blue*) in the absence of DYRK1A did not influence the cellular localization of DCAF7/WDR68 (Fig 8C, *green*), which agrees with the observation that FAM53C did not directly bind to DCAF7/WDR68 in the co-immunoprecipitation assays (Fig 6). The same conclusion was obtained when we switched the tags. 3xFLAG-DCAF7/WDR68, when expressed alone, localized both in the cytoplasm and the nucleus (Fig 8E, *blue*), and co-expression of HA-DYRK1A (accumulated in the nucleus as shown in Fig 8F, *magenta*) induced nuclear co-localization of DCAF7/WDR68 (Fig 8F, blue) with DYRK1A. Concurrent expression of GFP-FAM53C resulted in cytoplasmic co-localization of both DYRK1A (Fig 8H, *magenta*) and DCAF7/WDR68 (Fig 8H, *blue*) with FAM53C (Fig 8H, *green*). This result again indicates that FAM53C abrogates the ability of DYRK1A to anchor DCAF7/WDR68 in the nucleus. Taken altogether, it is concluded that DYRK1A tethers DCAF7/WDR68 and FAM53C by binding both of them, and that FAM53C anchors DYRK1A and DYRK1A-associated DCAF7/WDR68 in the cytoplasm.

Binding of FAM53C and Hsp90/Cdc37 to DYRK1B

The amino acid sequence identity is highest (85%) in the protein kinase catalytic domains of DYRK1A and DYRK1B, and FAM53C binds to the protein kinase domain of DYRK1A (Fig 4). We have previously shown that DYRK1B (but not DYRK1A) makes a stable complex with cellular molecular chaperone Hsp90 and its co-chaperone Cdc37 (Miyata & Nishida, 2021), and the Hsp90/Cdc37 chaperone system has been implicated in the maturation process of DYRK1B (Abu Jhaisha et al, 2017; Papenfuss et al, 2022). Hsp90/Cdc37 recognizes the catalytic kinase domains of various protein kinases, thus, we next examined the mutual relationship of DYRK1B-binding between Hsp90/Cdc37 and FAM53C. The binding of FAM53C to DYRK1B was examined by co-immunoprecipitation experiments in the presence or absence of an Hsp90-specific inhibitor Geldanamycin. Treatment of cells with Geldanamycin abolished the binding of both Hsp90 (Fig 9C, compare *lanes 5 & 6, lanes 7 & 8*) and Cdc37 (Fig 9D, compare *lanes 5 & 6, lanes 7 & 8*) to DYRK1B, in agreement with our previous investigation (Miyata & Nishida, 2021). Even after the complete disruption of Hsp90/Cdc37-DYRK1B binding, the amount of DYRK1B-associated FAM53C was not affected (Fig 9B, compare *lanes 7 & 8*). In addition, overexpression of FAM53C did not disrupt the binding of Hsp90 and Cdc37 to DYRK1B (Figs 9C & 9D, *lane 7*). We observed less Hsp90 and Cdc37 in the DYRK1B complexes from FAM53C-overexpressing

cells, however, this may be due to the decreased levels of expressed and immunoprecipitated DYRK1B by the dual expression with FAM53C (Figs 9A & 9E, compare *lanes 5 and 7*), and quantification and normalization with DYRK1B levels indicated that the amounts of associated Hsp90/Cdc37 per DYRK1B was not significantly affected by the overexpression of FAM53C. The amounts of GFP-FAM53C, Hsp90, and Cdc37 in the cell extracts were shown in Fig 9F, 9G, and 9H, respectively. These results indicate that Hsp90/Cdc37 binding is not required for the FAM53C binding to DYRK1B and that Hsp90/Cdc37 does not compete with FAM53C for binding to DYRK1B. The binding of Hsp90/Cdc37 and FAM53C may require different parts in the protein kinase domain of DYRK1B and is mutually independent.

Discussion

Tethering function and the protein interaction network of DYRK1A

DCAF7/WDR68 is the most major binding partner for DYRK1A (Glenewinkel et al, 2016; Miyata & Nishida, 2011; Yu et al, 2019). Our phospho-proteomic analysis identified FAM53C as a protein that makes a complex with DCAF7/WDR68 (Miyata & Nishida, 2021). Two other proteomic approaches have suggested FAM53C as a DYRK1A-interactor (Roewenstrunk et al, 2019) (Guard et al, 2019). These results indicate that FAM53C associates in cells with DYRK1A and/or DCAF7/WDR68. In this study, we directly show that DYRK1A binds to both FAM53C and DCAF7/WDR68 simultaneously with its different regions on the molecule. Whereas FAM53C bound to the protein kinase domain of DYRK1A (Fig. 4), DCAF7/WDR68 binds to the N-terminal domain of DYRK1A (Glenewinkel et al, 2016; Miyata & Nishida, 2011). DCAF7/WDR68 did not bind directly to FAM53C, but DYRK1A induced the association between DCAF7/WDR68 and FAM53C by binding to both of them, forming the DCAF7/WDR68-DYRK1A-FAM53C tri-protein complex. This result therefore indicates that our identification of FAM53C in the affinity-purified DCAF7/WDR68 complex should be due to the binding of FAM53C to DCAF7/WDR68 through endogenous DYRK1A in cells.

DYRK1A has been shown to associate in cells through DCAF7/WDR68 with several proteins including MEKK1 (Ritterhoff et al, 2010), adenovirus E1A (Glenewinkel et al, 2016), and IRS1(Frendo-Cumbo et al, 2022). In these cases, DCAF7/WDR68 works as a scaffold to stimulate the protein-protein interaction between otherwise non-interacting partners. DCAF7/WDR68 is a WD40-repeat protein with a ring structure consisted of seven beta-propellers, and proteins with this structure often function as bases for protein-protein interactions (Stirnimann et al, 2010). On the other hand, our findings in this study indicate that DYRK1A can also work as a scaffold to facilitate protein-protein interactions. Therefore, the DYRK1A-DCAF7/WDR68 pair assembles many proteins using both DYRK1A and DCAF7/WDR68, making this complex an important and efficient hub for many protein-protein interactions. Elucidation of the whole DYRK1A protein network should be fundamental for understanding the physiological function of DYRK1A in neurodevelopment and neurofunction at the molecular level.

We and others previously showed that DYRK1B, but not DYRK1A, makes stable complex with a set of molecular chaperones, including Hsp90, its co-chaperone Cdc37, and Hsp70 (Abu Jhaisha et al, 2017; Miyata & Nishida, 2021; Papenfuss et al, 2022). Hsp90/Cdc37 recognizes the catalytic domains of client protein kinases as in the case of FAM53C, thus the relationship between the binding of FAM53C and Hsp90/Cdc37 matters. Theoretically, FAM53C may bind to DYRK1B through Hsp90/Cdc37, however, this possibility may be unlikely, because DYRK1A, which does not make a stable complex with Hsp90/Cdc37, still binds to FAM53C. In addition, the complete dissociation of Hsp90/Cdc37 from DYRK1B by the Geldanamycin treatment did not abolish nor enhance the binding of FAM53C to

DYRK1B (Fig 9), indicating that the Hsp90 binding to DYRK1B is dispensable and permissive for the FAM53C binding.

FAM53C phosphorylation

Our phospho-proteomic analysis identified nine phosphorylation sites in FAM53C (Fig. 1A), and all of them are on serines (Ser86, Ser122, Ser162, Ser234, Ser247, Ser255, Ser273, Ser299, and Ser350). Results by high throughput phospho-proteomic analyses in the PhosphoSite database (https://www.phosphosite.org/proteinAction.action?id=6364) indicate that all the phosphoserines identified in this study, except pSer-350, can be observed in human, mouse, and rat. In addition, the PhosphoSite database indicates that pSer122, pSer162, and pSer232 are sensitive to Torin1 (an inhibitor for mTOR), AZD1152/ZM447439 (inhibitors for Aurora kinase) / BI2536 (an inhibitor for PLK1), and Dasatinib (an inhibitor for tyrosine kinases including Src and BCR-Abl), respectively. It remains unclear if FAM53C is a direct substrate of these kinases in cells. Four of the identified phosphorylation sites (pSer86, pSer162, pSer234, and pSer255) are immediately followed by a proline, suggesting that these sites of FAM53C might be phosphorylated by certain proline-directed protein kinases. Among them, the amino acid sequence surrounding pSer86 (RGNpSPKE) matches the DYRK1A substrate consensus sequence (RXXpSP) (Aranda et al, 2011; Himpel et al, 2000). Therefore, DYRK1A binds to, and may also phosphorylate FAM53C in cells. The amino acid sequences surrounding pSer122 (RSLpSVP) and pSer273 (RSRpSQP) are consistent with the consensus sequence motif (RXXpSXP) for phospho-dependent 14-3-3 binding (Pennington et al, 2018). In fact, the BioPlex interactome database (Fig 1B, *lower left panel*) suggests interactions of FAM53C with several 14-3-3 proteins including YWHAB(14-3-3β), YWHAG(14-3-3γ), YWHAH(14-3-3η), YQHAQ(14-3-3θ), and YWHAZ(14-3-3ζ). 14-3-3 proteins interact with numerous structurally and functionally diverse targets and act as central hubs of cellular signaling networks (Pennington et al, 2018). DYRK1A may therefore participate in a wide varieties of 14-3-3 dependent cellular signaling pathways through FAM53C binding. In fact, a very recent proteomic interactome study with all 14-3-3 human paralogs shows interaction of DYRK1A and FAM53C with five and six members out of seven 14-3-3 proteins (Segal et al, 2023). The possible functional importance of the serine phosphorylation of FAM53C identified in this study in physiological roles of DYRK1A will be a matter for future investigation.

FAM53C may function to keep DYRK1A in a kinase-inactive state in the cytoplasm

Trisomization of DYRK1A gene is responsible for many pathological phenotypes observed in Down syndrome patients. Therefore, the regulation of DYRK1A function is of physiological and clinical importance. Many low molecular weight compounds have been developed in the past decade as specific DYRK1A inhibitors (Arbones et al, 2019; Duchon & Hérault, 2016; Feki & Hibaoui, 2018; Kumar et al, 2021; Stotani et al, 2016), however, only few endogenous proteins such as RanBPM and SPREAD (Li et al, 2010; Zou et al, 2003) have been proposed to work inhibitory to DYRK1A. Here in this study, we

revealed that FAM53C suppresses the protein kinase activity of DYRK1A by binding to its catalytic domain. The suppression was observed both in phosphorylation of a well-established DYRK1A substrate MAPT/Tau and in autophosphorylation of DYRK1A itself. DYRK1A-dependent MAPT/Tau phosphorylation is one of the molecular bases for the early onset of Alzheimer disease in majority of Down syndrome patients (Ryoo et al, 2007) and DYRK1A inhibition is believed to be effective for treatment of Alzheimer disease (Branca et al, 2017; Stotani et al, 2016). FAM53C, by suppressing DYRK1A activity, may possibly also be involved in Alzheimer disease. DYRK1A is known to autophosphorylate on a tyrosine residue in the activation loop and this autophosphorylation is required for its maturation and full activity (Himpel et al, 2001; Lochhead et al, 2005). However, the autophosphorylation shown in this study is different from the tyrosine-autophosphorylation, because the tyrosine autophosphorylation is a one-off event during the translational process and the FAM53C-sensitive autophosphorylation was observed in a post-maturation stage during the incubation of affinity-purified DYRK1A with Mg^{2+}-ATP *in vitro*. The binding of FAM53C may interfere with the access of ATP or substrates to DYRK1A, or inactivate DYRK1A kinase by inducing its conformational alteration. Structural analysis of the FAM53C-DYRK1A complex may shed light on the molecular mechanism of the DYRK1A inhibition by FAM53C.

DYRK1A encodes a bipartite nuclear localization signal in the N-terminal domain and accumulate in the nucleus when exogenously over-expressed in various cell lines (Álvarez et al, 2003; Becker et al, 1998; Miyata & Nishida, 2011). However, many studies with various antibodies against DYRK1A have indicated that endogenous DYRK1A resides within the cytoplasm of brain tissues and in cell lines (Ferrer et al, 2005; Martí et al, 2003; Wegiel et al, 2004). This discrepancy have suggested that there may be an unveiled molecular mechanism responsible for anchoring DYRK1A in the cytoplasm. DYRK1A regulates gene expression by phosphorylating nuclear substrates. For example, DYRK1A-dependent phosphorylation of a transcription factor NFAT, which regulates immuno-responsive, inflammatory, and developmental processes, induces its cytoplasmic re-localization (Arron et al, 2006; Gwack et al, 2006). DYRK1A is also involved in transcriptional regulation by interacting with histone acetyl transferase p300 and CBP (Li et al, 2018) and by phosphorylating the C-terminal domain repeat of RNA polymerase II (Yu et al, 2019). Our results indicated that FAM53C binds to DYRK1A and keeps DYRK1A inactive in the cytoplasm, suggesting that FAM53C prevents DYRK1A from phosphorylating nuclear substrates. FAM53C is localized in the cytoplasm, and as the amounts of FAM53C in cells increases, DYRK1A remains in the cytoplasm with FAM53C to a greater extent (Fig 7). In the endogenous situation in vivo, DYRK1A and FAM53C levels remain in physiological balance, therefore, FAM53C can finely regulate the intracellular distribution of DYRK1A, appropriately keeping DYRK1A in the cytoplasm until needed. If DYRK1A is overexpressed beyond the available endogenous FAM53C level, the excess FAM53C-free DYRK1A may translocate into the cell nucleus and aberrantly phosphorylate nuclear proteins, leading to modified gene expression (Fig. 10). This may be one of the reasons why a mere 1.5-fold overexpression

of DYRK1A can induce drastic changes in gene expression and pathophysiological consequences in Down syndrome patients. FAM53C knock-out mice do not reproduce all the DYRK1A trisomy phenotypes, indicating the involvement of other molecular mechanisms, such as post-translational modifications or the binding of other interacting partners, in the regulation of DYRK1A activity and localization.

In conclusion, this study identified FAM53C as a binding protein of DYRK1A. DYRK1A concurrently bound to both FAM53C and DCAF7/WDR68 via its kinase domain and N-terminal domain, respectively, forming a tri-protein complex. FAM53C binding suppressed the protein kinase activity of DYRK1A towards MAPT/Tau and its own autophosphorylation, anchoring the DYRK1A-DCAF7/WDR68 complex in the cytoplasm in an inactive state. The amount of FAM53C in cells determined the appropriate intracellular distribution of DYRK1A and DCAF7/WDR68. Additionally, FAM53C bound to DYRK1B in an Hsp90/Cdc37-independet manner. These results explain in part why endogenous DYRK1A in animal brain tissues is often observed in the cytoplasm despite the strong tendency of DYRK1A nuclear localization. The identification of FAM53C as a suppressive anchoring partner for DYRK1A provides a crucial insight into the molecular mechanism of Down syndrome caused by triplication of DYRK1A in human chromosome 21.

Materials and Methods

Reagents and antibodies

An antibody specific for FAM53C was raised in a rabbit against a KLH-conjugated peptide, CQQDFGDLDLNLIEEN, corresponding to amino acids 377-392 (C-terminal end) of orangutan FAM53C. The antiserum was purified on an affinity column with the antigen peptide-conjugated resin. The peptide synthesis, immunization, and affinity purification were performed at Cosmo Bio Co., Ltd. Anti-FLAG antibody (M2), anti-FLAG (M2)-affinity resin, 3xFLAG peptide, and 3xFLAG-CMV7.1 vector were from Sigma, anti-GFP antibody (JL8) was from Clontech, and anti-Cdc37 antibody (E-4) was from SantaCruz. Anti-HA antibodies were from Roche (clone 12CA5 for Western blotting) or from SantaCruz (clone Y11 for immunofluorescent staining). Anti-Hsp90 antibody (Koyasu et al, 1986) and anti-DCAF7/WDR68 antibody (Miyata & Nishida, 2011) were described before. Geldanamycin was purchased from Life Technologies Inc. or from InvivoGen and stock solution was prepared at 5 mM in DMSO. pcDNA3-HA and pEGFP-C1Not vectors were previously described (Miyata et al, 1999; Miyata & Nishida, 2011; Miyata & Nishida, 2021). Hoechst 33342 was from Molecular Probes.

Isolation of human FAM53C cDNA

A cDNA fragment encoding human FAM53C was isolated by amplifying with nested PCR from human cDNA library plasmid (Takara). The oligonucleotide primer sequences used for the 1st PCR are 5′-CAAAGTGTGCAAGTCAAATCCTGG-3′ (5′ upstream) and 5′-CGGCTGGTTCTTTCCGCCTC-3′ (antisense primer in the vector region). The oligonucleotide primer sequences used for the 2nd PCR are 5′-GCGGCCGCTATGATAACCCTGATCACTGAG-3′ (*Not* I + 1st Met) and 5′-GCGGCCGCTTAGTTTTCCTCAATCAAATTC-3′ (3’ end + *Not* I, antisense). As a result, the amplified PCR fragment of FAM53C coding region contains a *Not* I site immediately 5′ upstream of the starting ATG and another *Not* I site 3′ downstream of the stop codon. The obtained PCR fragment was inserted into pCR2.1 Topo vector (Invitrogen) and the whole coding region was verified by direct sequencing. The *Not* I fragment encoding the entire FAM53C coding region was purified by low-melting gel electrophoresis. In the NCBI nucleotide database, three transcription variants are found for human FAM53C and we obtained isoform 1 (392 amino acids) with our cloning strategy.

Mammalian expression vectors for DYRK1A, DYRK1B, and FAM53C

Expression plasmids for 3xFLAG-tagged DYRK1A(WT), DYRK1A(N), DYRK1A(K), DYRK1A(C), DYRK1A(N+K), DYRK1A(K+C), and DYRK1B(WT) were previously described (Miyata & Nishida, 2011; Miyata & Nishida, 2021). *Not* I fragments encoding the N-terminal (N), the kinase domain (K), and the N-terminal domain+the kinase domain (N+K) of DYRK1A were ligated into the *Not* I site of pEGFPC1Not to obtain plasmids of GFP-fusion proteins for DYRK1A(N), DYRK1A(K), and DYRK1A(N+K), respectively. HA-DYRK1A expression plasmid was previously described (Miyata &

Nishida, 2011). The *Not* I fragment of FAM53C was ligated into the *Not* I site of p3xFLAG-CMV7.1 or pEGFP-C1Not to obtain plasmids for expression of 3xFLAG-tagged or GFP-tagged FAM53C.

Expression in mammalian cells and immunoprecipitation experiments

COS7 and NIH-3T3 cells were cultured in DMEM supplemented with 10% FCS at 37°C. Cells were transfected with mammalian expression vectors by electroporation as described previously (Miyata et al, 1999; Miyata et al, 1997), or by lipofection with Lipofectamine LTX plus or with Lipofectamine 2000 according to the protocol supplied by the manufacture. Cell extracts were prepared as described before (Miyata et al, 1999; Miyata et al, 1997). Extracts with equal amounts of proteins were incubated with 10 μl of anti-FLAG resin for 12h at 4°C. The immunocomplexes were washed, isolated, and FLAG-tagged proteins were eluted and analyzed as described previously (Miyata et al, 2001; Miyata & Nishida, 2004).

Immunofluorescent staining

COS7 and NIH-3T3 cells were transfected with plasmids encoding GFP-, 3xFLAG-, or HA-tagged proteins and cultured in 35mm dishes on glass cover slips. 24 hours later, cells were fixed with 10% formaldehyde (37°C 20 min), stained with anti-FLAG- or anti-HA antibody, and observed with a fluorescent microscope (Axiophot, Zeiss, or IX71, Olympus) essentially as described (Miyata & Nishida, 2004; Miyata & Nishida, 2021). For staining of the nuclei, cells were incubated with 1 μg/ml of Hoechst 33342, 3% BSA, 0.1% goat IgG in PBS at room temperature for 60 min. All the immunofluorescent staining experiments were repeated with consistent results, and typical representative cell images are shown.

In vitro DYRK1A protein kinase assay

The protein kinase activity of DYRK1A was determined *in vitro* with recombinant MAPT/Tau protein as an exogenous substrate. A DNA fragment encoding human full length hT40 MAPT/Tau was obtained by PCR with plasmid DNA encoding wild-type full-length hT40 MAPT/Tau as a template. The oligonucleotide primer sequences used are 5′-GCGGCCGCCATGGCTGAGCCCCGCCAGGAG-3′ (*Not* I + 1st Met) and 5′- GCGGCCGCTCACAAACCCTGCTTGGCCAG-3′ (3’ end + *Not* I, antisense). As a result, the amplified PCR fragment of MAPT/Tau coding region contains a *Not* I site immediately 5′ upstream of the starting ATG and another *Not* I site 3′ downstream of the stop codon. The *Not* I fragment was verified by direct sequencing and inserted into the *Not* I site of pGEX6P2 (Cytiva), and the expression vector was introduced into an *Escherichia coli* strain BL21-CodonPlus (DE3)-RIL (Agilent). The transformed bacterial cells were grown at 37°C until OD600 reached 0.7, and isopropyl-β-D-thiogalactopyranoside (IPTG) was added at a final concentration of 0.5 mM to induce the expression of GST-MAPT/Tau followed by 2h incubation at 22°C. The bacterial cells were collected by a centrifugation (7,000 *g* 15 min 2°C), washed once with cold PBS, frozen at -80°C, and solubilized in B-PER solution (Pierce) supplemented with 1/100 (v/v) of bacterial protease inhibitor cocktail (Sigma), 1

mM EDTA, and 0.5 M NaCl. The extract was clarified by a centrifugation (18,000 *g* 15 min 2°C) and mixed with glutathione-Sepharose (Cytiva) for 4h followed by three times washes with PBS + TritonX100 (1%) and three times washes with cleavage buffer (50 mM Tris, 150 mM NaCl, 1 mM EDTA 1 mM DTT, pH 7.0). The GST moiety of the fusion protein was removed by incubating with PreScission protease (Cytiva) for 12h at 4°C, and released MAPT/Tau protein was purified with HiTrap CM Sepharose FF (Cytiva) with a NaCl gradient (50-1,000 mM) in purification buffer (50 mM MES, 1 mM DTT, 1 mM EDTA, pH 6.4). Eluted fractions containing MAPT/Tau protein were collected, desalted with a PD10 column (Cytiva) to 50 mM NaCl in the purification buffer, and concentrated by an Amicon Ultra-15 filter unit (30,000Da cut-off, Millipore). The recombinant MAPT/Tau protein was >98% pure as revealed by CBB staining.

3xFLAG-DYRK1A expressed in COS7 cells was affinity-purified as described above and incubated with purified recombinant MAPT/Tau protein for 30 min at 30°C with gentle shaking for phosphorylation reactions. Composition of the reaction mixture (20 μL) was 50 mM Hepes, 10 mM Tris, 1.25 mM MES, 81.25 mM NaCl, 2% glycerol, 10 mM $MgCl_2$, 5 mM ATP, 0.2% NP40, 0.225 mM DTT, 0.425 mM EDTA, pH 7.4, containing 0.35 μg (17.5 μg/mL) MAPT/Tau. The reactions were stopped by adding SDS-sample buffer followed by an incubation at 98°C for 5 min. DYRK1A-dependent phosphorylation of Thr212 of MAPT/Tau protein was evaluated by Western blotting with anti-phospho Tau (Thr212) antibody (Invitrogen, #44740G).

Other procedures

Sodium dodecyl sulfate-polyacrylamide gel electrophoresis (SDS-PAGE) was performed with 8% or 10% acrylamide gels and BOLT MES (Invitrogen) or Tris-glycine SDS running buffer. Western blotting was performed using polyvinylidene difluoride (PVDF) filter membranes (Millipore) for electro-transfer and Blocking One (Nacalai Tesque) for blocking. Signals were developed with horseradish peroxidase-conjugated secondary antibodies (GE Healthcare Bio-sciences) or peroxidase-conjugated primary antibodies using Western Lightning Plus-ECL (PerkinElmer) and the chemiluminescent system AI680 (GE Healthcare) as described (Miyata & Nishida, 2004). In some experiments, PVDF membrane wetting was performed with ethanol instead of methanol, and we confirmed that this does not affect the results. For all the Western blotting data, we repeated independent experiments and showed representative images of obtained consistent results.

Data availability

This study does not contain deposited data in external repositories. Original data can be provided upon request.

Acknowledgements

We thank T. Sakabe, T. Aoki, and M. Nakagawa for their excellent technical assistance. We thank Drs. B. Chambraud and E. E. Baulieu (INSERM U1195, France) for providing us plasmid DNA encoding human hT40 MAPT/Tau. This work was supported by Grants-in-Aid for Scientific Research from the Ministry of Education, Culture, Sports, Science and Technology of Japan.

Author contributions

Yoshihiko Miyata: Conceptualization, methodology, investigation, visualization, project administration, funding acquisition, writing –original draft, writing – review & editing.

Eisuke Nishida: Supervision, project administration, funding acquisition, resource, writing – review and editing.

Disclosure and competing interests statement

The authors declare that they have no conflict of interest.

References

Abu Jhaisha S, Widowati EW, Kii I, Sonamoto R, Knapp S, Papadopoulos C, Becker W (2017) DYRK1B mutations associated with metabolic syndrome impair the chaperone-dependent maturation of the kinase domain. *Sci Rep* **7:** 6420

Altafaj X, Dierssen M, Baamonde C, Martí E, Visa J, Guimerà J, Oset M, González JR, Flórez J, Fillat C *et al.* (2001) Neurodevelopmental delay, motor abnormalities and cognitive deficits in transgenic mice overexpressing *Dyrk1A* (*minibrain*), a murine model of Down's syndrome. *Hum Mol Genet* **10:** 1915-1923

Alvarez M, Altafaj X, Aranda S, de la Luna S (2007) DYRK1A autophosphorylation on serine residue 520 modulates its kinase activity via 14-3-3 binding. *Mol Biol Cell* **18:** 1167-1178

Álvarez M, Estivill X, de la Luna S (2003) DYRK1A accumulates in splicing speckles through a novel targeting signal and induces speckle disassembly. *J Cell Sci* **116:** 3099-3107

Aranda S, Laguna A, de la Luna S (2011) DYRK family of protein kinases: evolutionary relationships, biochemical properties, and functional roles. *FASEB J* **25:** 449-462

Arbones ML, Thomazeau A, Nakano-Kobayashi A, Hagiwara M, Delabar JM (2019) DYRK1A and cognition: A lifelong relationship. *Pharmacol Ther* **194:** 199-221

Arron JR, Winslow MM, Polleri A, Chang CP, Wu H, Gao X, Neilson JR, Chen L, Heit JJ, Kim SK *et al.* (2006) NFAT dysregulation by increased dosage of DSCR1 and DYRK1A on chromosome 21. *Nature* **441:** 595-600

Becker W, Joost H-G (1999) Structural and functional characteristics of Dyrk, a novel subfamily of protein kinases with dual specificity. *Prog Nucleic Acid Res Mol Biol* **62:** 1-17

Becker W, Sippl W (2011) Activation, regulation, and inhibition of DYRK1A. *FEBS J* **278:** 246-256

Becker W, Weber Y, Wetzel K, Eirmbter K, Tejedor FJ, Joost H-G (1998) Sequence characteristics, subcellular localization, and substrate specificity of DYRK-related kinases, a novel family of dual specificity protein kinases. *J Biol Chem* **273:** 25893-25902

Bhansali RS, Rammohan M, Lee P, Laurent AP, Wen Q, Suraneni P, Yip BH, Tsai YC, Jenni S, Bornhauser B *et al.* (2021) DYRK1A regulates B cell acute lymphoblastic leukemia through phosphorylation of FOXO1 and STAT3. *J Clin Invest* **131:** e135937

Blazek JD, Abeysekera I, Li J, Roper RJ (2015) Rescue of the abnormal skeletal phenotype in Ts65Dn Down syndrome mice using genetic and therapeutic modulation of trisomic Dyrk1a. *Hum Mol Genet* **24:** 5687-5696

Branca C, Shaw DM, Belfiore R, Gokhale V, Shaw AY, Foley C, Smith B, Hulme C, Dunckley T, Meechoovet B *et al.* (2017) Dyrk1 inhibition improves Alzheimer's disease-like pathology. *Aging Cell* **16:** 1146-1154

Bronicki LM, Redin C, Drunat S, Piton A, Lyons M, Passemard S, Baumann C, Faivre L, Thevenon J, Rivière JB *et al.* (2015) Ten new cases further delineate the syndromic intellectual disability phenotype

caused by mutations in DYRK1A. *Eur J Hum Genet* **23:** 1482-1487

Courraud J, Chater-Diehl E, Durand B, Vincent M, Del Mar Muniz Moreno M, Boujelbene I, Drouot N, Genschik L, Schaefer E, Nizon M *et al.* (2021) Integrative approach to interpret DYRK1A variants, leading to a frequent neurodevelopmental disorder. *Genet Med* **23:** 2150-2159

De Rubeis S, He X, Goldberg AP, Poultney CS, Samocha K, Cicek AE, Kou Y, Liu L, Fromer M, Walker S *et al.* (2014) Synaptic, transcriptional and chromatin genes disrupted in autism. *Nature* **515:** 209-215

Di Vona C, Bezdan D, Islam AB, Salichs E, López-Bigas N, Ossowski S, de la Luna S (2015) Chromatin-wide profiling of DYRK1A reveals a role as a gene-specific RNA polymerase II CTD kinase. *Mol Cell* **57:** 506-520

Dirice E, Walpita D, Vetere A, Meier BC, Kahraman S, Hu J, Dančík V, Burns SM, Gilbert TJ, Olson DE *et al.* (2016) Inhibition of DYRK1A Stimulates Human beta-Cell Proliferation. *Diabetes* **65:** 1660-1671

Dowjat K, Adayev T, Kaczmarski W, Wegiel J, Hwang YW (2012) Gene dosage-dependent association of DYRK1A with the cytoskeleton in the brain and lymphocytes of down syndrome patients. *J Neuropathol Exp Neurol* **71:** 1100-1112

Duchon A, Hérault Y (2016) DYRK1A, a dosage-sensitive gene involved in neurodevelopmental disorders, is a target for drug development in Down syndrome. *Front Behav Neurosci* **10:** 104

Feki A, Hibaoui Y (2018) DYRK1A Protein, A Promising Therapeutic Target to Improve Cognitive Deficits in Down Syndrome. *Brain Sci* **8**

Ferrer I, Barrachina M, Puig B, Martínez de Lagrán M, Martí E, Avila J, Dierssen M (2005) Constitutive Dyrk1A is abnormally expressed in Alzheimer disease, Down syndrome, Pick disease, and related transgenic models. *Neurobiol Dis* **20:** 392-400

Frendo-Cumbo S, Li T, Ammendolia DA, Coyaud E, Laurent EMN, Liu Y, Bilan PJ, Polevoy G, Raught B, Brill JA *et al.* (2022) DCAF7 regulates cell proliferation through IRS1-FOXO1 signaling. *iScience* **25:** 105188

Galceran J, de Graaf K, Tejedor FJ, Becker W (2003) The Mnb/Dyrk1A protein kinase: genetic and biochemical properties. *J Neural Transm Suppl* **67:** 139-148

Glenewinkel F, Cohen MJ, King CR, Kaspar S, Bamberg-Lemper S, Mymryk JS, Becker W (2016) The adaptor protein DCAF7 mediates the interaction of the adenovirus E1A oncoprotein with the protein kinases DYRK1A and HIPK2. *Sci Rep* **6:** 28241

Guard SE, Poss ZC, Ebmeier CC, Pagratis M, Simpson H, Taatjes DJ, Old WM (2019) The nuclear interactome of DYRK1A reveals a functional role in DNA damage repair. *Sci Rep* **9:** 6539

Gwack Y, Sharma S, Nardone J, Tanasa B, Iuga A, Srikanth S, Okamura H, Bolton D, Feske S, Hogan PG *et al.* (2006) A genome-wide *Drosophila* RNAi screen identifies DYRK-family kinases as regulators of NFAT. *Nature* **441:** 646-650

Hämmerle B, Elizalde C, Galceran J, Becker W, Tejedor FJ (2003) The Mnb/Dyrk1A protein kinase: neurobiological functions and Down syndrome implications. *J Neural Transm Suppl* **67:** 129-137

Himpel S, Panzer P, Eirmbter K, Czajkowska H, Sayed M, Packman LC, Blundell T, Kentrup H, Grötzinger J, Joost HG *et al.* (2001) Identification of the autophosphorylation sites and characterization of their effects in the protein kinase DYRK1A. *Biochem J* **359:** 497-505

Himpel S, Tegge W, Frank R, Leder S, Joost HG, Becker W (2000) Specificity determinants of substrate recognition by the protein kinase DYRK1A. *J Biol Chem* **275:** 2431-2438

Huttlin EL, Bruckner RJ, Navarrete-Perea J, Cannon JR, Baltier K, Gebreab F, Gygi MP, Thornock A, Zarraga G, Tam S *et al.* (2021) Dual proteome-scale networks reveal cell-specific remodeling of the human interactome. *Cell* **184:** 3022-3040.e3028

Huttlin EL, Bruckner RJ, Paulo JA, Cannon JR, Ting L, Baltier K, Colby G, Gebreab F, Gygi MP, Parzen H *et al.* (2017) Architecture of the human interactome defines protein communities and disease networks. *Nature* **545:** 505-509

Iossifov I, Levy D, Allen J, Ye K, Ronemus M, Lee YH, Yamrom B, Wigler M (2015) Low load for disruptive mutations in autism genes and their biased transmission. *Proc Natl Acad Sci USA* **112:** E5600-5607

Ji J, Lee H, Argiropoulos B, Dorrani N, Mann J, Martinez-Agosto JA, Gomez-Ospina N, Gallant N, Bernstein JA, Hudgins L *et al.* (2015) DYRK1A haploinsufficiency causes a new recognizable syndrome with microcephaly, intellectual disability, speech impairment, and distinct facies. *Eur J Hum Genet* **23:** 1473-1481

Kim OH, Cho HJ, Han E, Hong TI, Ariyasiri K, Choi JH, Hwang KS, Jeong YM, Yang SY, Yu K *et al.* (2017) Zebrafish knockout of Down syndrome gene, DYRK1A, shows social impairments relevant to autism. *Mol Autism* **8:** 50

Kimura R, Kamino K, Yamamoto M, Nuripa A, Kida T, Kazui H, Hashimoto R, Tanaka T, Kudo T, Yamagata H *et al.* (2007) The DYRK1A gene, encoded in chromosome 21 Down syndrome critical region, bridges between beta-amyloid production and tau phosphorylation in Alzheimer disease. *Hum Mol Genet* **16:** 15-23

Koyasu S, Nishida E, Kadowaki T, Matsuzaki F, Iida K, Harada F, Kasuga M, Sakai H, Yahara I (1986) Two mammalian heat shock proteins, HSP90 and HSP100, are actin-binding proteins. *Proc Natl Acad Sci USA* **83:** 8054-8058

Kumar K, Suebsuwong C, Wang P, Garcia-Ocaña A, Stewart AF, DeVita RJ (2021) DYRK1A Inhibitors as Potential Therapeutics for beta-Cell Regeneration for Diabetes. *J Med Chem* **64:** 2901-2922

Li D, Jackson RA, Yusoff P, Guy GR (2010) Direct Association of Sprouty-related Protein with an EVH1 Domain (SPRED) 1 or SPRED2 with DYRK1A Modifies Substrate/Kinase Interactions. *J Biol Chem* **285:** 35374-35385

Li S, Xu C, Fu Y, Lei PJ, Yao Y, Yang W, Zhang Y, Washburn MP, Florens L, Jaiswal M *et al.* (2018) DYRK1A interacts with histone acetyl transferase p300 and CBP and localizes to enhancers. *Nucleic Acids Res* **46:** 11202-11213

Liu F, Liang Z, Wegiel J, Hwang YW, Iqbal K, Grundke-Iqbal I, Ramakrishna N, Gong CX (2008)

Overexpression of Dyrk1A contributes to neurofibrillary degeneration in Down syndrome. *FASEB J* **22:** 3224-3233

Lochhead PA, Sibbet G, Morrice N, Cleghon V (2005) Activation-loop autophosphorylation is mediated by a novel transitional intermediate form of DYRKs. *Cell* **121:** 925-936

Lu H, Yu D, Hansen AS, Ganguly S, Liu R, Heckert A, Darzacq X, Zhou Q (2018) Phase-separation mechanism for C-terminal hyperphosphorylation of RNA polymerase II. *Nature* **558:** 318-323

Martí E, Altafaj X, Dierssen M, de la Luna S, Fotaki V, Alvarez M, Pérez-Riba M, Ferrer I, Estivill X (2003) Dyrk1A expression pattern supports specific roles of this kinase in the adult central nervous system. *Brain Res* **964:** 250-263

Mazmanian G, Kovshilovsky M, Yen D, Mohanty A, Mohanty S, Nee A, Nissen RM (2010) The zebrafish *dyrk1b* gene is important for endoderm formation. *Genesis* **48:** 20-30

McElyea SD, Starbuck JM, Tumbleson-Brink DM, Harrington E, Blazek JD, Ghoneima A, Kula K, Roper RJ (2016) Influence of prenatal EGCG treatment and Dyrk1a dosage reduction on craniofacial features associated with Down syndrome. *Hum Mol Genet* **25:** 4856-4869

Menon VR, Ananthapadmanabhan V, Swanson S, Saini S, Sesay F, Yakovlev V, Florens L, DeCaprio JA, Washburn MP, Dozmorov M *et al.* (2019) DYRK1A regulates the recruitment of 53BP1 to the sites of DNA damage in part through interaction with RNF169. *Cell Cycle* **18:** 531-551

Miyata Y, Akashi M, Nishida E (1999) Molecular cloning and characterization of a novel member of the MAP kinase superfamily. *Genes Cells* **4:** 299-309

Miyata Y, Chambraud B, Radanyi C, Leclerc J, Lebeau M-C, Renoir J-M, Shirai R, Catelli M-G, Yahara I, Baulieu E-E (1997) Phosphorylation of the immunosuppressant FK506-binding protein FKBP52 by casein kinase II (CK2): Regulation of HSP90-binding activity of FKBP52. *Proc Natl Acad Sci USA* **94:** 14500-14505

Miyata Y, Ikawa Y, Shibuya M, Nishida E (2001) Specific association of a set of molecular chaperones including HSP90 and Cdc37 with MOK, a member of the MAP kinase superfamily. *J Biol Chem* **276:** 21841-21848

Miyata Y, Nishida E (1999) Distantly related cousins of MAP kinase: Biochemical properties and possible physiological functions. *Biochem Biophys Res Commun* **266:** 291-295

Miyata Y, Nishida E (2004) CK2 controls multiple protein kinases by phosphorylating a kinase-targeting molecular chaperone Cdc37. *Mol Cell Biol* **24:** 4065-4074

Miyata Y, Nishida E (2011) DYRK1A binds to an evolutionarily conserved WD40-repeat protein WDR68 and induces its nuclear translocation. *Biochim Biophys Acta-Mol Cell Res* **1813:** 1728-1739

Miyata Y, Nishida E (2021) Protein quality control of DYRK family protein kinases by the Hsp90-Cdc37 molecular chaperone. *Biochim Biophys Acta-Mol Cell Res* **1868:** 119081

Miyata Y, Shibata T, Aoshima M, Tsubata T, Nishida E (2014) The molecular chaperone TRiC/CCT binds to the Trp-Asp 40 (WD40) repeat protein WDR68 and promotes its folding, protein kinase DYRK1A binding, and nuclear accumulation. *J Biol Chem* **289:** 33320-33332

Morita K, Lo Celso C, Spencer-Dene B, Zouboulis CC, Watt FM (2006) HAN11 binds mDia1 and controls GLI1 transcriptional activity. *J Dermatol Sci* **44:** 11-20

O'Roak BJ, Vives L, Girirajan S, Karakoc E, Krumm N, Coe BP, Levy R, Ko A, Lee C, Smith JD *et al.* (2012) Sporadic autism exomes reveal a highly interconnected protein network of de novo mutations. *Nature* **485:** 246-250

Ori-McKenney KM, McKenney RJ, Huang HH, Li T, Meltzer S, Jan LY, Vale RD, Wiita AP, Jan YN (2016) Phosphorylation of beta-Tubulin by the Down Syndrome Kinase, Minibrain/DYRK1a, Regulates Microtubule Dynamics and Dendrite Morphogenesis. *Neuron* **90:** 551-563

Papenfuss M, Lützow S, Wilms G, Babendreyer A, Flaßhoff M, Kunick C, Becker W (2022) Differential maturation and chaperone dependence of the paralogous protein kinases DYRK1A and DYRK1B. *Sci Rep* **12:** 2393

Park J, Song WJ, Chung KC (2009) Function and regulation of Dyrk1A: towards understanding Down syndrome. *Cell Mol Life Sci* **66:** 3235-3240

Pennington KL, Chan TY, Torres MP, Andersen JL (2018) The dynamic and stress-adaptive signaling hub of 14-3-3: emerging mechanisms of regulation and context-dependent protein-protein interactions. *Oncogene* **37:** 5587-5604

Rachdi L, Kariyawasam D, Aïello V, Herault Y, Janel N, Delabar JM, Polak M, Scharfmann R (2014) Dyrk1A induces pancreatic beta cell mass expansion and improves glucose tolerance. *Cell Cycle* **13:** 2221-2229

Ritterhoff S, Farah CM, Grabitzki J, Lochnit G, Skurat AV, Schmitz ML (2010) The WD40-repeat protein Han11 functions as a scaffold protein to control HIPK2 and MEKK1 kinase functions. *EMBO J* **29:** 3750-3761

Roewenstrunk J, Di Vona C, Chen J, Borras E, Dong C, Arató K, Sabidó E, Huen MSY, de la Luna S (2019) A comprehensive proteomics-based interaction screen that links DYRK1A to RNF169 and to the DNA damage response. *Sci Rep* **9:** 6014

Ryoo SR, Jeong HK, Radnaabazar C, Yoo JJ, Cho HJ, Lee HW, Kim IS, Cheon YH, Ahn YS, Chung SH *et al.* (2007) DYRK1A-mediated hyperphosphorylation of Tau. A functional link between Down syndrome and Alzheimer disease. *J Biol Chem* **282:** 34850-34857

Scales TM, Lin S, Kraus M, Goold RG, Gordon-Weeks PR (2009) Nonprimed and DYRK1A-primed GSK3 beta-phosphorylation sites on MAP1B regulate microtubule dynamics in growing axons. *J Cell Sci* **122:** 2424-2435

Schweppe DK, Huttlin EL, Harper JW, Gygi SP (2018) BioPlex Display: An Interactive Suite for Large-Scale AP-MS Protein-Protein Interaction Data. *J Proteome Res* **17:** 722-726

Segal D, Maier S, Mastromarco GJ, Qian WW, Nabeel-Shah S, Lee H, Moore G, Lacoste J, Larsen B, Lin ZY *et al.* (2023) A central chaperone-like role for 14-3-3 proteins in human cells. *Mol Cell* **83:** 974-993 e915

Shen W, Taylor B, Jin Q, Nguyen-Tran V, Meeusen S, Zhang YQ, Kamireddy A, Swafford A, Powers AF,

Walker J *et al.* (2015) Inhibition of DYRK1A and GSK3B induces human beta-cell proliferation. *Nat Commun* **6:** 8372

Skurat AV, Dietrich AD (2004) Phosphorylation of Ser640 in muscle glycogen synthase by DYRK family protein kinases. *J Biol Chem* **279:** 2490-2498

Stirnimann CU, Petsalaki E, Russell RB, Müller CW (2010) WD40 proteins propel cellular networks. *Trends Biochem Sci* **35:** 565-574

Stotani S, Giordanetto F, Medda F (2016) DYRK1A inhibition as potential treatment for Alzheimer's disease. *Future Med Chem* **8:** 681-696

Tian T, Zhang Y, Wu T, Yang L, Chen C, Li N, Li Y, Xu S, Fu Z, Cui X *et al.* (2019) miRNA profiling in the hippocampus of attention-deficit/hyperactivity disorder rats. *J Cell Biochem* **120:** 3621-3629

van Bon BW, Coe BP, Bernier R, Green C, Gerdts J, Witherspoon K, Kleefstra T, Willemsen MH, Kumar R, Bosco P *et al.* (2016) Disruptive de novo mutations of DYRK1A lead to a syndromic form of autism and ID. *Mol Psychiatry* **21:** 126-132

Varjosalo M, Keskitalo S, Van Drogen A, Nurkkala H, Vichalkovski A, Aebersold R, Gstaiger M (2013) The protein interaction landscape of the human CMGC kinase group. *Cell Rep* **3:** 1306-1320

Wang P, Alvarez-Perez JC, Felsenfeld DP, Liu H, Sivendran S, Bender A, Kumar A, Sanchez R, Scott DK, Garcia-Ocaña A *et al.* (2015) A high-throughput chemical screen reveals that harmine-mediated inhibition of DYRK1A increases human pancreatic beta cell replication. *Nat Med* **21:** 383-388

Wegiel J, Dowjat K, Kaczmarski W, Kuchna I, Nowicki K, Frackowiak J, Mazur Kolecka B, Wegiel J, Silverman WP, Reisberg B *et al.* (2008) The role of overexpressed DYRK1A protein in the early onset of neurofibrillary degeneration in Down syndrome. *Acta Neuropathol* **116:** 391-407

Wegiel J, Gong CX, Hwang YW (2011) The role of DYRK1A in neurodegenerative diseases. *FEBS J* **278:** 236-245

Wegiel J, Kuchna I, Nowicki K, Frackowiak J, Dowjat K, Silverman WP, Reisberg B, DeLeon M, Wisniewski T, Adayev T *et al.* (2004) Cell type- and brain structure-specific patterns of distribution of minibrain kinase in human brain. *Brain Res* **1010:** 69-80

Yu D, Cattoglio C, Xue Y, Zhou Q (2019) A complex between DYRK1A and DCAF7 phosphorylates the C-terminal domain of RNA polymerase II to promote myogenesis. *Nucleic Acids Res* **47:** 4462-4475

Zhou X, Feliciano P, Shu C, Wang T, Astrovskaya I, Hall JB, Obiajulu JU, Wright JR, Murali SC, Xu SX *et al.* (2022) Integrating de novo and inherited variants in 42,607 autism cases identifies mutations in new moderate-risk genes. *Nat Genet* **54:** 1305-1319

Zou Y, Lim S, Lee K, Deng X, Friedman E (2003) Serine/threonine kinase Mirk/Dyrk1B is an inhibitor of epithelial cell migration and is negatively regulated by the Met adaptor Ran-binding protein M. *J Biol Chem* **278:** 49573-49581

Figure legends

Figure 1. Identification of FAM53C as an interactor candidate for DCAF7/WDR68 and DYRK1A

A. Phospho-proteomic analysis of binding proteins of DCAF7/WDR68 exogenously expressed in COS7 cells identified nine phosphopeptides (underlined orange boxes) corresponding to FAM53C. The amino acid sequence of human FAM53C is shown with identified phosphorylation sites (shown in green with amino acid numbers).

B. BioPlex protein-protein interaction network analysis. The database was analyzed with DYRK1A (*upper panels*, in HEK293T [*left*] or HCT116 [*right*]), DCAF7/WDR68 (*middle panels*, in HEK293T [*left*] or HCT116 [*right*]), FAM53C (*lower left panel* in HEK293T), and DYRK1B (*lower right panel* in HEK293T) as queries (located in the center of the networkgrams). Identified interacting partners are shown and FAM53C (*orange*), DCAF7/WDR68 (*yellow*), DYRK1A (*blue*), and DYRK1B (*magenta*) are color-highlighted. Proteins with circles indicate baits, and proteins with diamonds indicate prey. The arrow heads show the bait-to-prey direction.

C. Structural characterization of FAM53C. Structural prediction of FAM53C by AlphaFold2 (*upper panel*) and the intrinsically disordered tendency score of FAM53C by IUPred2 (*lower panel*) are shown.

Figure 2. Association of FAM53C with DYRK1A and DYRK1B

DYRK1A and DYRK1B were expressed as 3xFLAG-tagged proteins with GFP-tagged FAM53C in COS7 cells. DYRK1A and DYRK1B were immunoprecipitated with resin conjugated with anti-FLAG antibody and protein complexes were analyzed by SDS-PAGE/Western blotting.

A. The amounts of DYRK1A, DYRK1B (*upper panel*), and FAM53C (*lower panel*) in the immunocomplexes were shown by Western blotting. *Lane 1*, Control; *lane 2*, DYRK1A; *lane 3*, DYRK1B.

B. The amounts of DYRK1A, DYRK1B (*upper panel*), and FAM53C (*lower panel*) in the extracts were shown by Western blotting. *Lane 1*, Control; *lane 2*, DYRK1A; *lane 3*, DYRK1B. FAM53C were transfected in *lanes 1-3*.

Figure 3. Binding of endogenous FAM53C with DYRK1A and DYRK1B

A. COS7 cells (*lane 1, control*) were transfected with 3xFLAG-FAM53C (*lane 2*) or GFP-FAM53C (*lane 3*). Total cell lysates were prepared and examined by Western blotting with indicated antibodies as follows. *Top left*, control pre-immune serum; *Top right*, C-terminal peptide-directed FAM53C

antibody (extracts in *lanes 2 & 3* in this panel were x100 diluted to avoid signal saturation. The asterisk indicates the position of full length endogenous FAM53C); *Bottom left*, anti-FLAG antibody, showing the expression of 3xFLAG-FAM53C; *Bottom right*, anti-GFP antibody, showing the expression of GFP-FAM53C.

B. COS7 cells were transfected with 3xFLAG-tagged DYRK1A or DYRK1B and the co-immunoprecipitation of endogenous FAM53C with DYRK1A and DYRK1B was examined by Western blotting. *Lane 1*, control IgG-immunoprecipitate from non-transfected control cells; *lane 2*, anti-FLAG immunoprecipitate from non-transfected control cells; *lane 3*, control IgG-immunoprecipitate from 3xFLAG-DYRK1A-transfected cells; *lane 4*, anti-FLAG-immunoprecipitate from 3xFLAG-DYRK1A-transfected cells; *lane 5*, control IgG-immunoprecipitate from 3xFLAG-DYRK1B-transfected cells; *lane 6*, anti-FLAG-immunoprecipitate from 3xFLAG-DYRK1B-transfected cells. Western blotting images with the anti-FAM53C antibody (*upper panels*) and with anti-FLAG antibody (*lower panels*) are shown.

Figure 4. Identification of the FAM53C binding domain in DYRK1A

3xFLAG-DYRK1A (wild type or deletion mutants) and GFP-FAM53C were expressed in COS7 cells and the binding of FAM53C to DYRK1A was examined by co-immunoprecipitation experiments. *Lane 1*, DYRK1A(WT); *lane 2*, DYRK1A(N); *lane 3*, DYRK1A(K); *lane 4*, DYRK1A(C); *lane 5*, DYRK1A(N+K); *lane 6*, DYRK1A(K+C).

A. Western blotting of immunoprecipitates with anti-GFP antibody for detection of DYRK1A-bound FAM53C.

B. Western blotting of immunoprecipitates with anti-FLAG antibody for detection of immunoprecipitated DYRK1A.

C. Expression levels of GFP-FAM53C in total cell lysates.

D. Expression levels of 3xFLAG-tagged wild type and deletion mutants of DYRK1A in total cell lysates.

Figure 5. Suppressive effect of the FAM53C binding on the kinase activity of DYRK1A

3xFLAG-DYRK1A was expressed in COS7 cells (*lanes 2, 3, 5, & 6*) with (*lanes 3 & 6*) or without (*lanes 1, 2, 4, & 5*) GFP-FAM53C and affinity purified. As controls, mock affinity purification with control resin (*lanes 1-3*) and affinity purification from non-transfected cell extracts (*lanes 1 & 4*) were included. *In vitro* DYRK1A protein kinase assay was conducted with recombinant MAPT/Tau protein as a substrate. In addition, Mg^{2+}/ATP requirements for the kinase reactions were examined (*lanes 7-10*). Purified recombinant MAPT/Tau was incubated with affinity purified DYRK1A with or without Mg^{2+} (10 mM)

and/or ATP (5 mM) as indicated on the top. DYRK1A-dependent phosphorylation of MAPT/Tau on Thr212 and DYRK1A electrophoretic mobilities were determined by Western blotting.

A. Anti-phospho-Tau (Thr212) Western blotting showing the DYRK1A kinase activity to an exogenous substrate MAPT/Tau.
B. CBB staining of the kinase reaction mixtures showing the amounts of MAPT/Tau protein.
C. Anti-FLAG Western blotting showing the amounts and electrophoretic mobilities of DYRK1A.
D. Anti-FAM53C Western blotting showing the association of overexpressed FAM53C with DYRK1A. Endogenous FAM53C was not visible at this exposure.
E. Anti-phospho-Tau (Thr212) Western blotting showing the DYRK1A kinase activity to an exogenous substrate MAPT/Tau.
F. CBB staining of the kinase reaction mixtures showing the amounts of MAPT/Tau protein.
G. Anti-FLAG Wester blotting showing the amounts and electrophoretic mobilities of DYRK1A.

Figure 6. DYRK1A-mediated association of FAM53C with DCAF7/WDR68

HA-DCAF7/WDR68 (*lanes 1-7*) and 3xFLAG-FAM53C (*lanes 3-7*) were expressed in COS7 cells with full length (*lanes 2 & 4*, DYRK1A), the N-terminal domain (*lane 5,* DYRK1A-N), the kinase domain (*lane 6*, DYRK1A-K), and N-terminal+kinase domain (*lane 7*, DYRK1A-NK) of GFP-tagged DYRK1A as indicated.

A. The amounts of immunoprecipitated FAM53C were shown by Western blotting with anti-FLAG antibody.
B. The association of DYRK1A with immunoprecipitated FAM53C was shown by Western blotting with anti-GFP antibody.
C. The association of DCAF7/WDR68 with immunoprecipitated FAM53C was shown by Western blotting with anti-HA antibody.
D. The amounts of total expressed FAM53C in cell extracts were shown by Western blotting with anti-FLAG antibody.
E. The amounts of wild type and deletion mutants of expressed DYRK1A in cell extracts were shown by Western blotting with anti-GFP antibody.
F. The amounts of total expressed DCAF7/WDR68 in cell extracts were shown by Western blotting (anti-DCAF7/WDR68 antibody was used for this panel due to non-specific signals observed with anti-HA antibody in the cell extracts).
G. The schematic illustration of the tethering function of DYRK1A observed in **A-C**. Expressed DCAF7/WDR68 (*yellow*), FAM53C (*red*), and DYRK1A [N-term (*green*), kinase (*blue*), and C-term (*pink*) domains] in the Input (total cell extracts) are shown (*right*). FAM53C, bound DYRK1A, and

tethered DCAF7/WDR68 in the FAM53C-immunocomplexes are indicated (*left*). Lane numbers correspond to the lanes shown in **A-F**.

Figure 7. FAM53C anchors DYRK1A in the cytoplasm

A-E. NIH-3T3 cells were transfected with GFP-FAM53C and/or 3xFLAG-DYRK1A. The intracellular distribution of FAM53C (*left panels, green*) and DYRK1A (*center panels, magenta*) was visualized by fluorescent microscopy. Concurrently, cells were stained with Hoechst 33342 for visualization of nucleus (*right panels, blue*). (A) Control without transfection; (B) GFP-FAM53C alone; (C) 3xFLAG-DYRK1A alone; (D) Both FAM53C and DYRK1A; (E) A merged image of D.

F-K. NIH-3T3 cells were transfected with 3xFLAG-FAM53C and/or GFP-DYRK1A. The intracellular distribution of FAM53C (*left panels, magenta*) and DYRK1A (*center panels, green*) was visualized by fluorescent microscopy. Concurrently, cells were stained with Hoechst 33342 for visualization of nucleus (*right panels, blue*). (F) 3xFLAG-FAM53C alone; (G) GFP-DYRK1A alone; (H-K) Both FAM53C and DYRK1A; (I) A merged image of H. (J, K) Two representative microscopic fields showing cells with different expression levels of FAM53C. The arrows indicate cells with high FAM53C expression and arrowheads indicate cells with low or no FAM53C expression.

Figure 8. Tethering function of DYRK1A to FAM53C and DCAF7/WDR68

A-D. NIH-3T3 cells were transfected with GFP-DCAF7/WDR68 (*green*), HA-DYRK1A (*magenta*), and 3xFLAG-FAM53C (*blue*) and the intracellular distribution of these proteins was examined by fluorescent microscopy. (A) DCAF7/WDR68 alone; (B) DCAF7/WDR68 and DYRK1A; (C) DCAF7/WDR68 and FAM53C; (D**)** DCAF7/WDR68, DYRK1A, and FAM53C.

E-H. NIH-3T3 cells were transfected with 3xFLAG-DCAF7/WDR68 (*blue*), HA-DYRK1A (*magenta*), and GFP-FAM53C (*green*), and the intracellular distribution of these proteins was examined by fluorescent microscopy. (E) DCAF7/WDR68 alone; (F) DCAF7/WDR68 and DYRK1A; (G) DCAF7/WDR68 and FAM53C; (H) DCAF7/WDR68, DYRK1A, and FAM53C.

Figure 9. Binding FAM53C and Hsp90/Cdc37 to DYRK1B

3xFLAG-DYRK1B (*lanes 5-8*) was expressed in COS7 cells with (*lanes 3, 4, 7, and 8*) or without (*lanes 1, 2, 5, and 6*) GFP-FAM53C. Cells were treated with (*lanes 2, 4, 6, and 8*) or without (vehicle DMSO, *lanes 1, 3, 5, and 7*) Geldanamycin (2.5 μM 4h), and the binding of FAM53C, Hsp90, and Cdc37 to DYRK1B was examined by co-immunoprecipitation experiments.

A. The amounts of immunoprecipitated DYRK1B were shown by Western blotting with anti-FLAG

antibody.

B. The amounts of FAM53C co-immunoprecipitated with DYRK1B were shown by Western blotting with anti-GFP antibody.

C. The amounts of Hsp90 co-immunoprecipitated with DYRK1B were shown by Western blotting with anti-Hsp90 antibody.

D. The amounts of Cdc37 co-immunoprecipitated with DYRK1B were shown by Western blotting with anti-Cdc37 antibody.

E-H. The levels of indicated proteins in the cell extracts were examined by Western blotting. (E) FLAG-DYRK1B; (F) GFP-FAM53C; (G) Hsp90; (H) Cdc37.

Figure 10. Schematic illustrations of the tethering function of DYRK1A and the suppressive anchoring function of FAM53C

A. A schematic illustration of the tri-protein complex formation of DYRK1A with DCAF7/WDR68 and FAM53C. DYRK1A concurrently binds to DCAF7/WDR68 and FAM53C with its N-terminal domain (N) and the catalytic protein kinase domain (K), respectively.

B. Regulation of the intracellular localization of DYRK1A by a balance between levels of DYRK1A and FAM53C. Sufficient amounts of FAM53C are required for the efficient anchoring of DYRK1A in the cytoplasm in an inactive state (*green area*). FAM53C-free DYRK1A is active and translocates into the cell nucleus with DCAF7/WDR68 (*red area*). In certain conditions, a 1.5-times increase of DYRK1A (shown by bars), by crossing over the balance threshold (shown by a boundary line), might induce a drastic change of intracellular distribution of DYRK1A from the cytoplasm (*green area*) to the nucleus (*red area*).

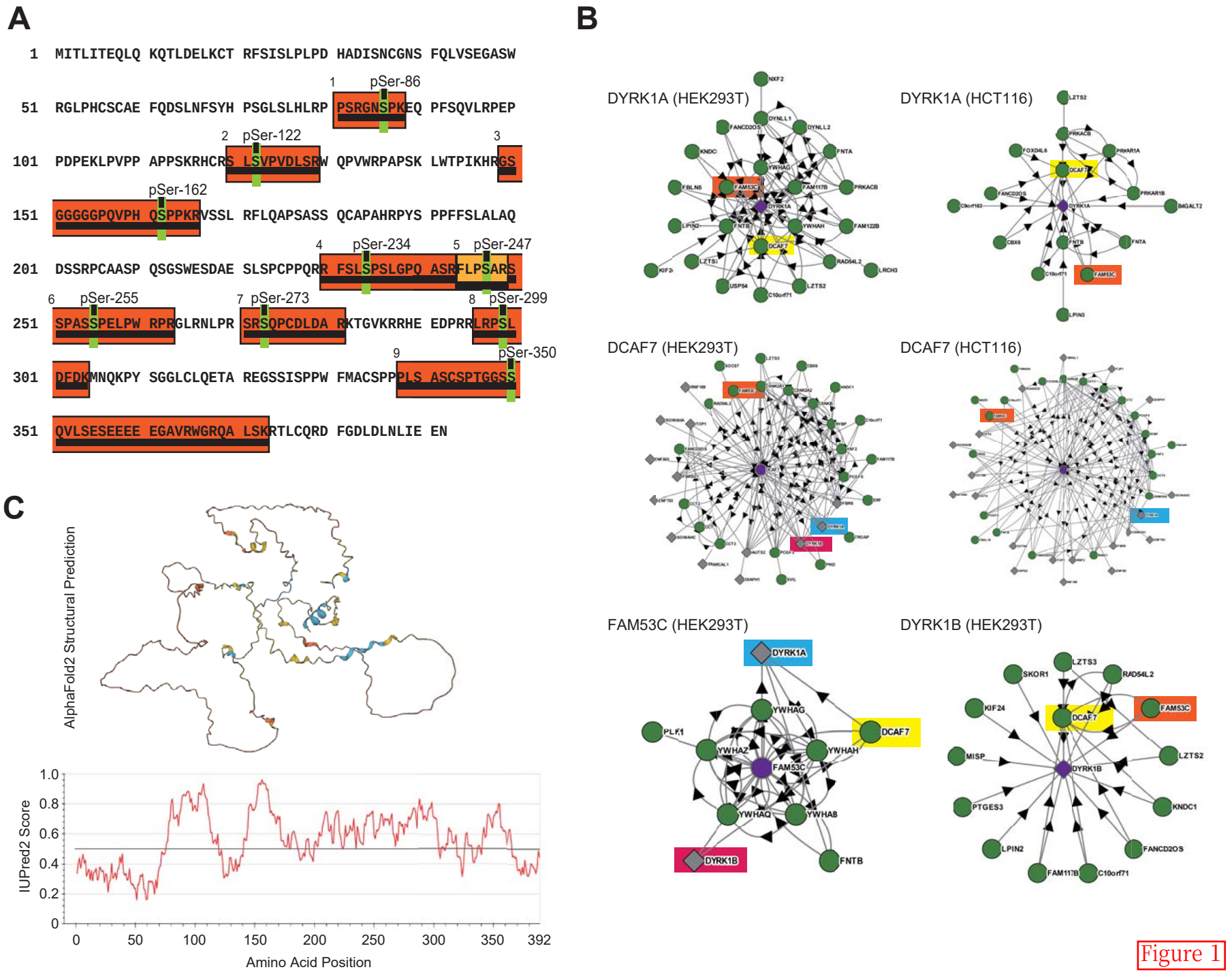
A
1 MITLITEQLQ KQTLDELKCT RFSISLPLPD HADISNCGNS FQLVSEGASW
1 pSer-86
51 RGLPHCSCAE FQDSLNFSYH PSGLSLHLRP PSRGNSPKEQ PFSQVLRPEP
2 pSer-122
3
101 PDPEKLPVPP APPSKRHCRS LSVPVDLSRW QPVWRPAPSK LWTPIKHRGS
pSer-162
151 GGGGGPQVPH QSPPKRVSSL RFLQAPSASS QCAPAHRPYS PPFFSLALAQ
4 pSer-234
5 pSer-247
201 DSSRPCAASP QSGSWESDAE SLSPCPPQRR FSLSPSLGPQ ASRFLPSARS
6 pSer-255
7 pSer-273
8 pSer-299
251 SPASSPELPW RPRGLRNLPR SRSQPCDLDA RKTGVKRRHE EDPRRLRPSL
9
pSer-350
301 DFDKMNQKPY SGGLCLQETA REGSSISPPW FMACSPPPLS ASCSPTGCSS
351 QVLSESEEEE EGAVRWGRQA LSKRTLCQRD FGDLDLNLIE EN
B
DYRK1A (HEK293T)
DYRK1A (HCT116)
DCAF7 (HEK293T)
DCAF7 (HCT116)
FAM53C (HEK293T)
DYRK1B (HEK293T)
C
AlphaFold2 Structural Prediction
IUPred2 Score
1.0
0.8
0.6
0.4
0.2
0
0
50
100
150
200
250
300
350
392
Amino Acid Position

Figure 1

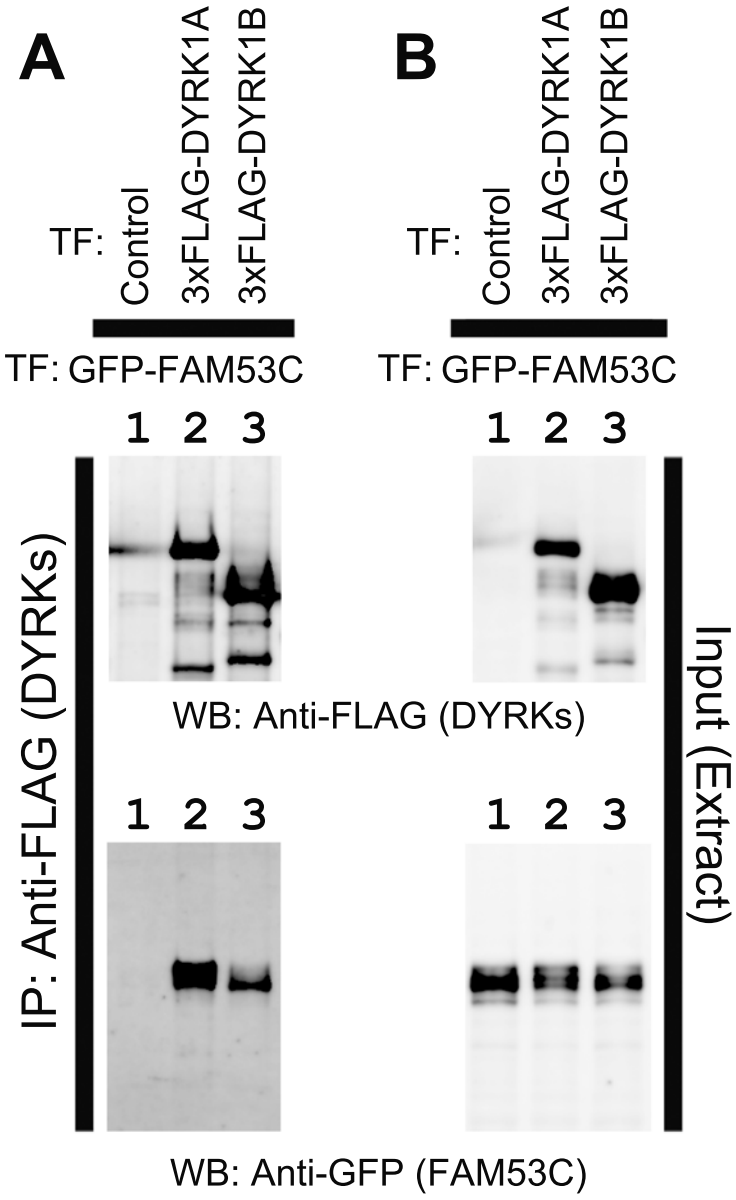
A
B
TF:
Control
3xFLAG-DYRK1A
3xFLAG-DYRK1B
TF: GFP-FAM53C
1 2 3
IP: Anti-FLAG (DYRKs)
Input (Extract)
WB: Anti-FLAG (DYRKs)
WB: Anti-GFP (FAM53C)

Figure 2

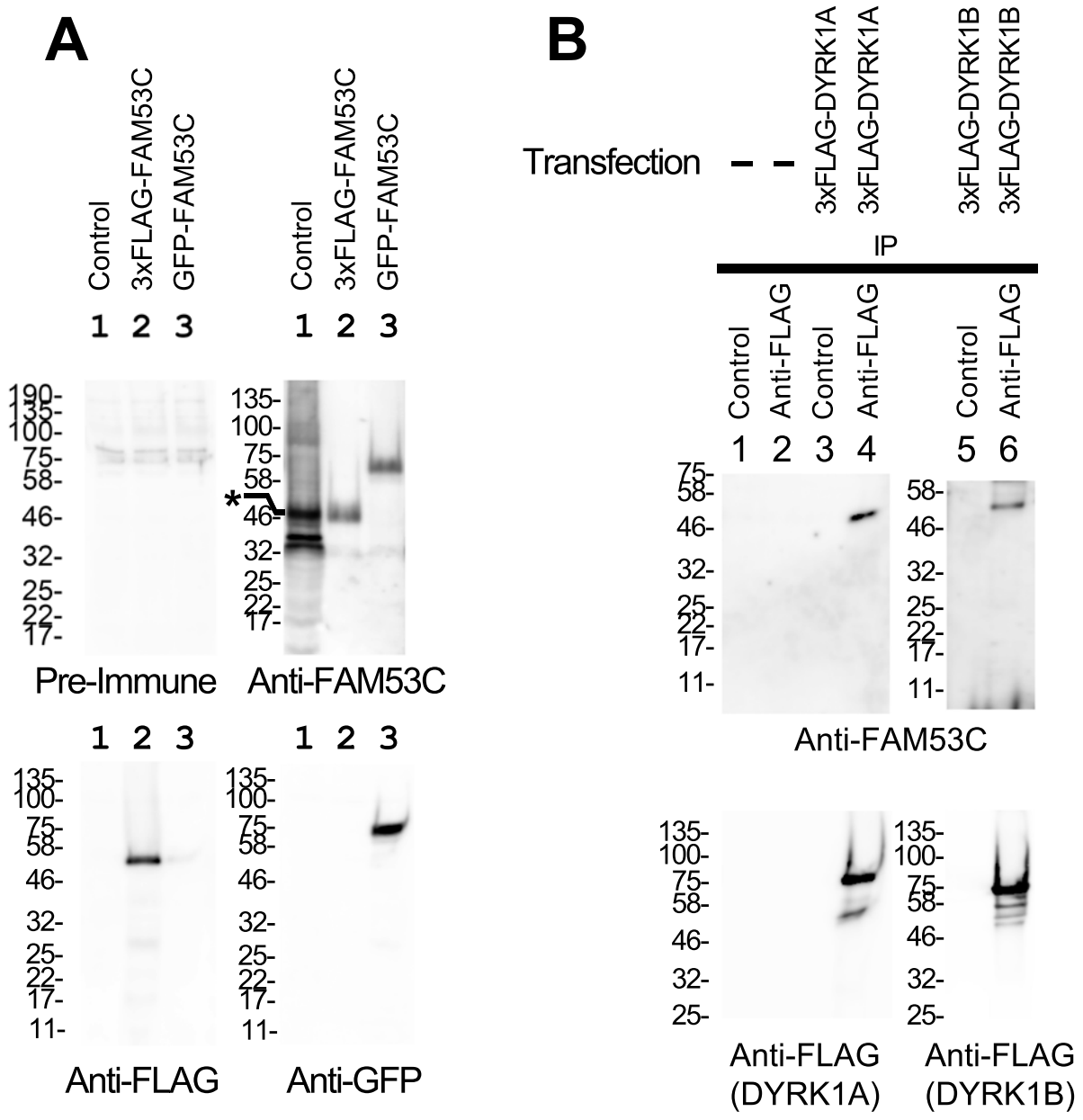
A
Control
3xFLAG-FAM53C
GFP-FAM53C
1 2 3
190-
135-
100-
75-
58-
46-
32-
25-
22-
17-
Pre-Immune
Anti-FAM53C
*
Anti-FLAG
Anti-GFP
11-
B
Transfection
3xFLAG-DYRK1A
3xFLAG-DYRK1B
IP
Control
Anti-FLAG
1 2 3 4 5 6
Anti-FAM53C
Anti-FLAG (DYRK1A)
Anti-FLAG (DYRK1B)

Figure 3

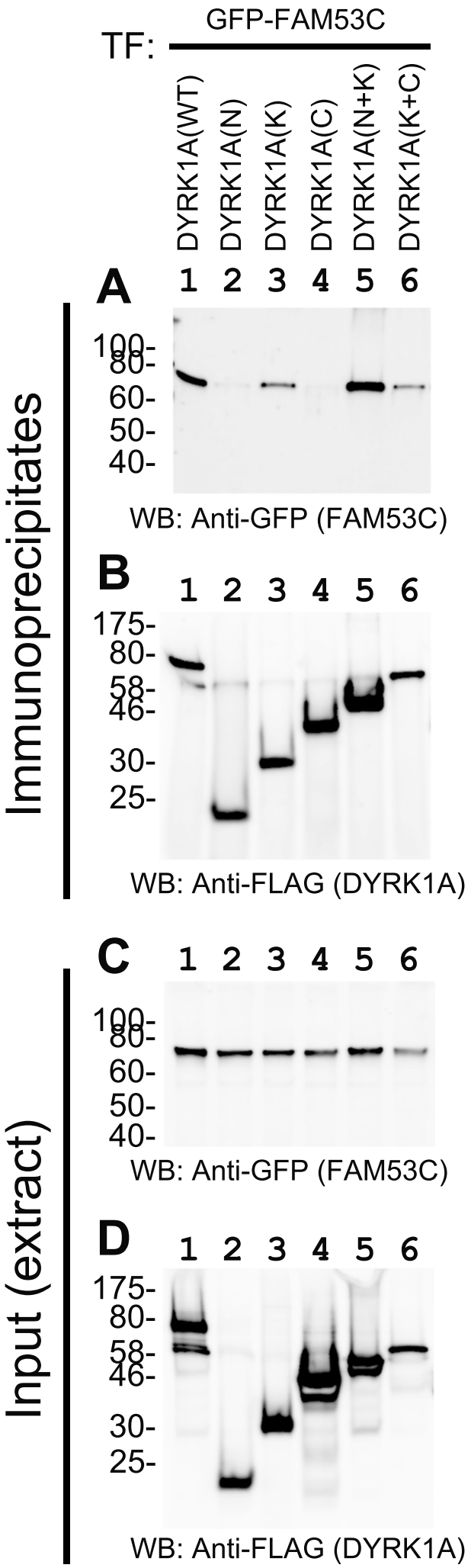
TF:
GFP-FAM53C
DYRK1A(WT)
DYRK1A(N)
DYRK1A(K)
DYRK1A(C)
DYRK1A(N+K)
DYRK1A(K+C)
A
1 2 3 4 5 6
100-
80-
60-
50-
40-
WB: Anti-GFP (FAM53C)
B
1 2 3 4 5 6
175-
80-
58-
46-
30-
25-
WB: Anti-FLAG (DYRK1A)
Immunoprecipitates
C
1 2 3 4 5 6
100-
80-
60-
50-
40-
WB: Anti-GFP (FAM53C)
D
1 2 3 4 5 6
175-
80-
58-
46-
30-
25-
WB: Anti-FLAG (DYRK1A)
Input (extract)

Figure 4

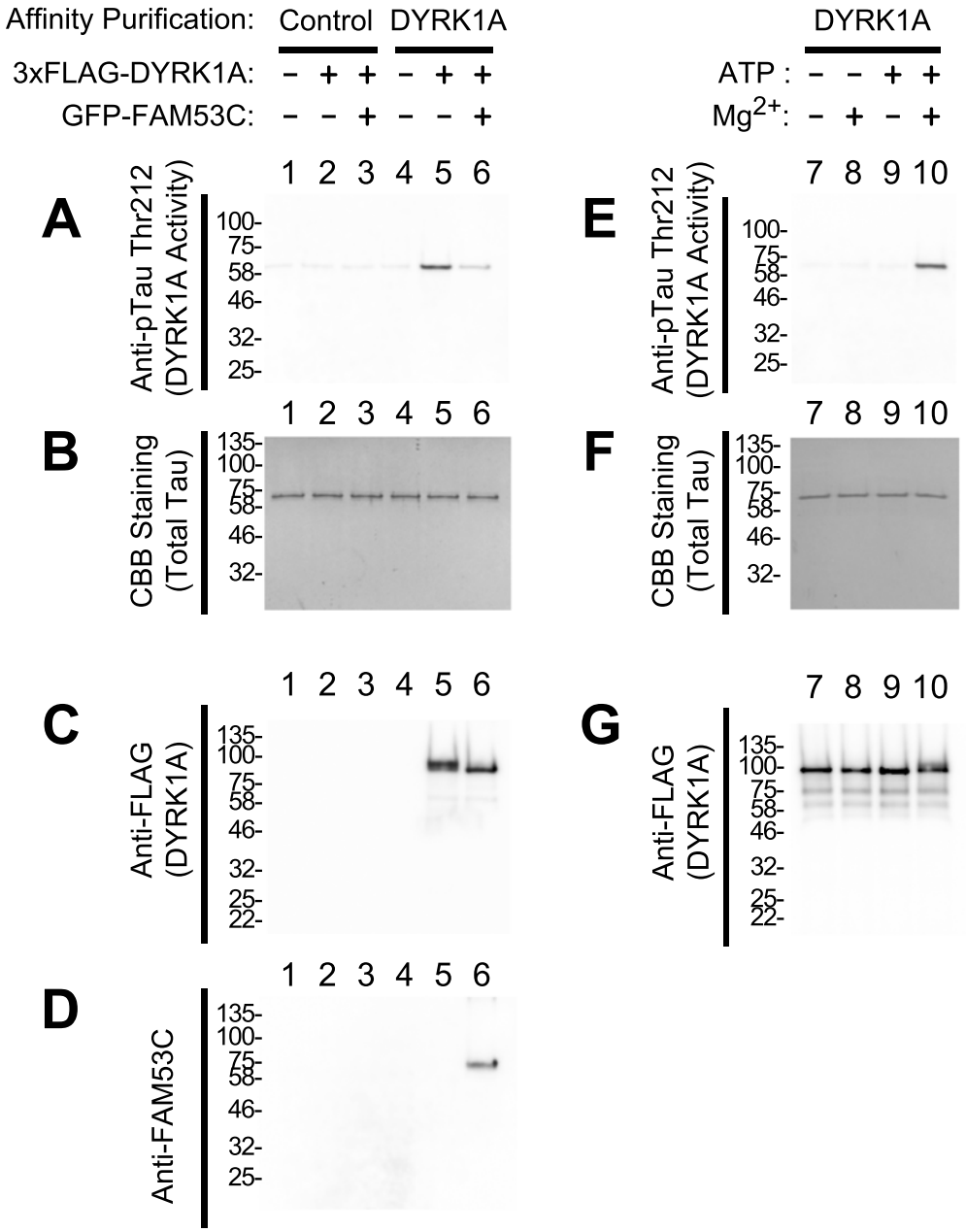
Affinity Purification: Control DYRK1A
3xFLAG-DYRK1A: − + + − + +
GFP-FAM53C: − − + − − +
DYRK1A
ATP : − − + +
Mg2+: − + − +
A
Anti-pTau Thr212 (DYRK1A Activity)
1 2 3 4 5 6
100- 75- 58- 46- 32- 25-
B
CBB Staining (Total Tau)
1 2 3 4 5 6
135- 100- 75- 58- 46- 32-
C
Anti-FLAG (DYRK1A)
1 2 3 4 5 6
135- 100- 75- 58- 46- 32- 25- 22-
D
Anti-FAM53C
1 2 3 4 5 6
135- 100- 75- 58- 46- 32- 25-
E
Anti-pTau Thr212 (DYRK1A Activity)
7 8 9 10
100- 75- 58- 46- 32- 25-
F
CBB Staining (Total Tau)
7 8 9 10
135- 100- 75- 58- 46- 32-
G
Anti-FLAG (DYRK1A)
7 8 9 10
135- 100- 75- 58- 46- 32- 25- 22-

Figure 5

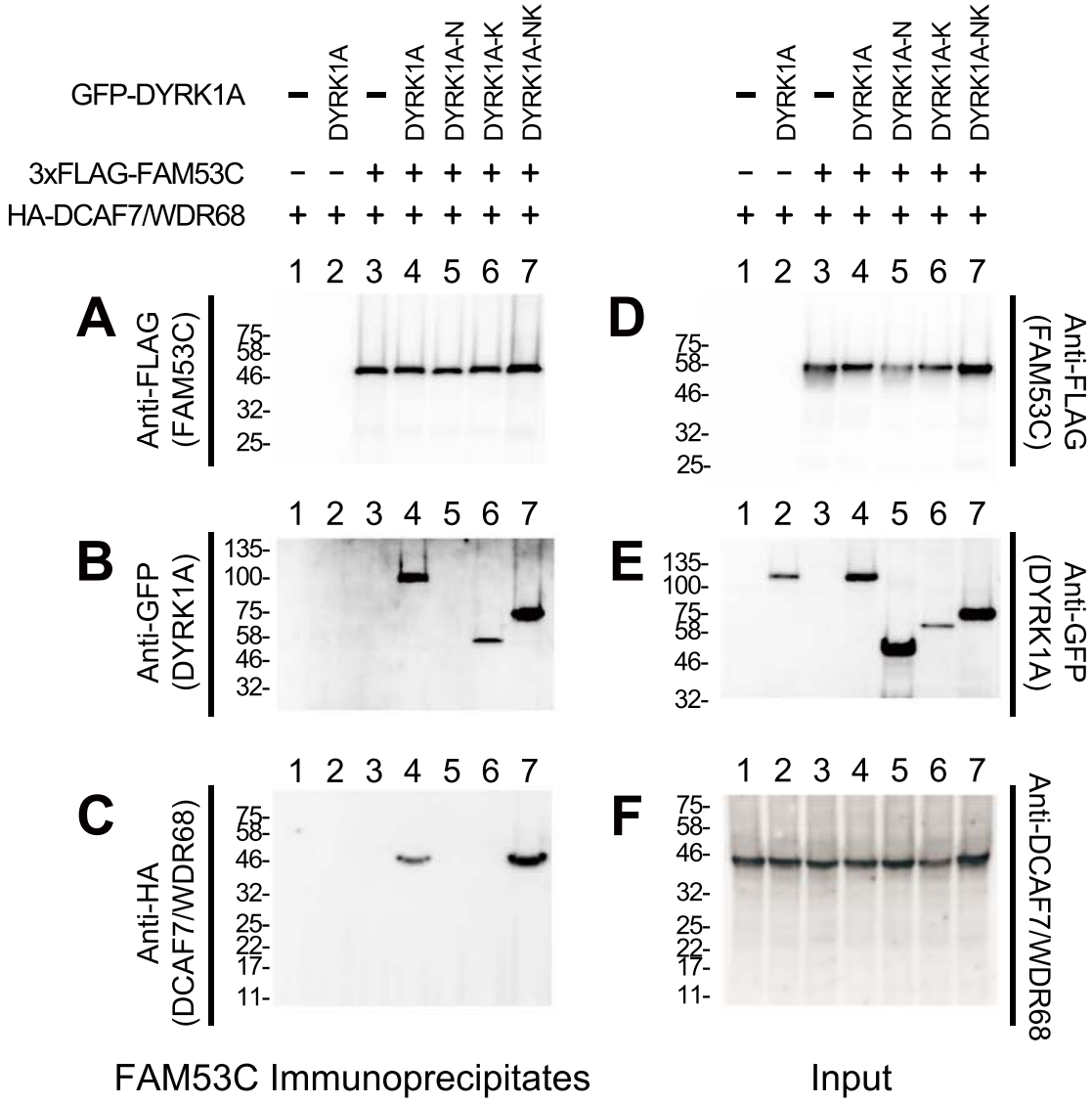
GFP-DYRK1A
3xFLAG-FAM53C
HA-DCAF7/WDR68
DYRK1A
DYRK1A-N
DYRK1A-K
DYRK1A-NK
1 2 3 4 5 6 7
A
Anti-FLAG (FAM53C)
75-
58-
46-
32-
25-
B
Anti-GFP (DYRK1A)
135-
100-
75-
58-
46-
32-
C
Anti-HA (DCAF7/WDR68)
75-
58-
46-
32-
25-
22-
17-
11-
D
Anti-FLAG (FAM53C)
E
Anti-GFP (DYRK1A)
F
Anti-DCAF7/WDR68
FAM53C Immunoprecipitates
Input

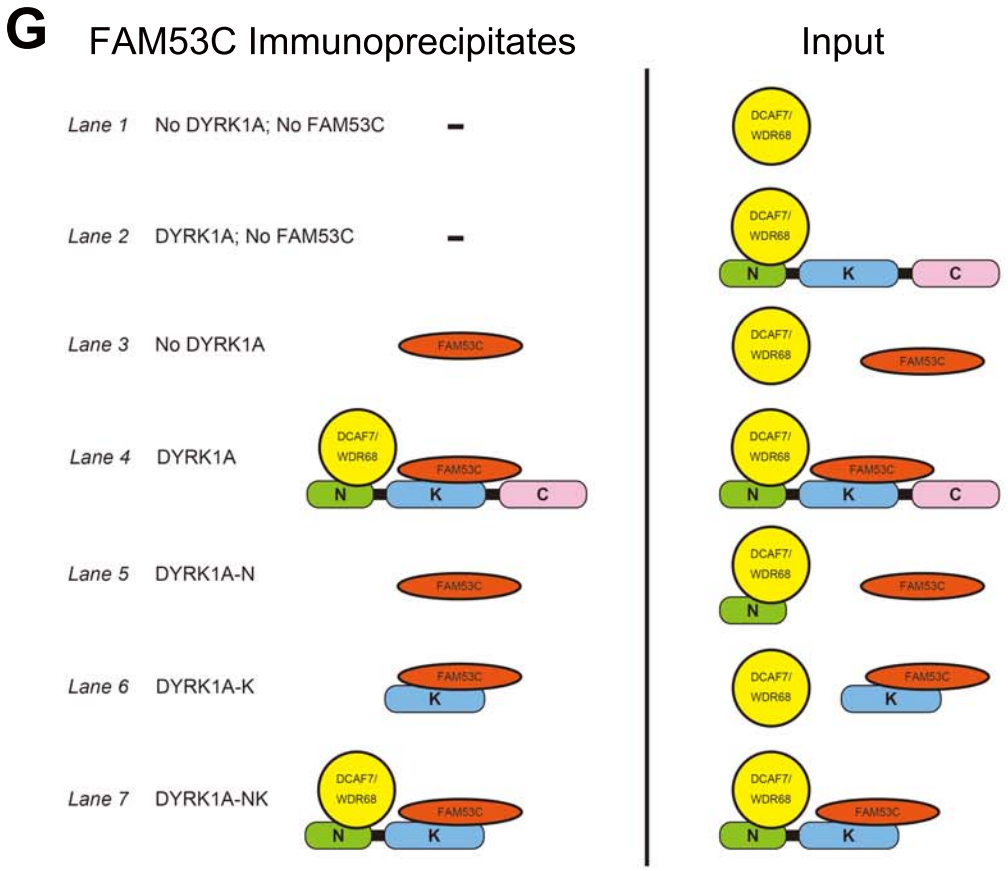
G
FAM53C Immunoprecipitates
Input
Lane 1 No DYRK1A; No FAM53C
Lane 2 DYRK1A; No FAM53C
Lane 3 No DYRK1A
Lane 4 DYRK1A
Lane 5 DYRK1A-N
Lane 6 DYRK1A-K
Lane 7 DYRK1A-NK
DCAF7/ WDR68
FAM53C
N
K
C

Figure 6

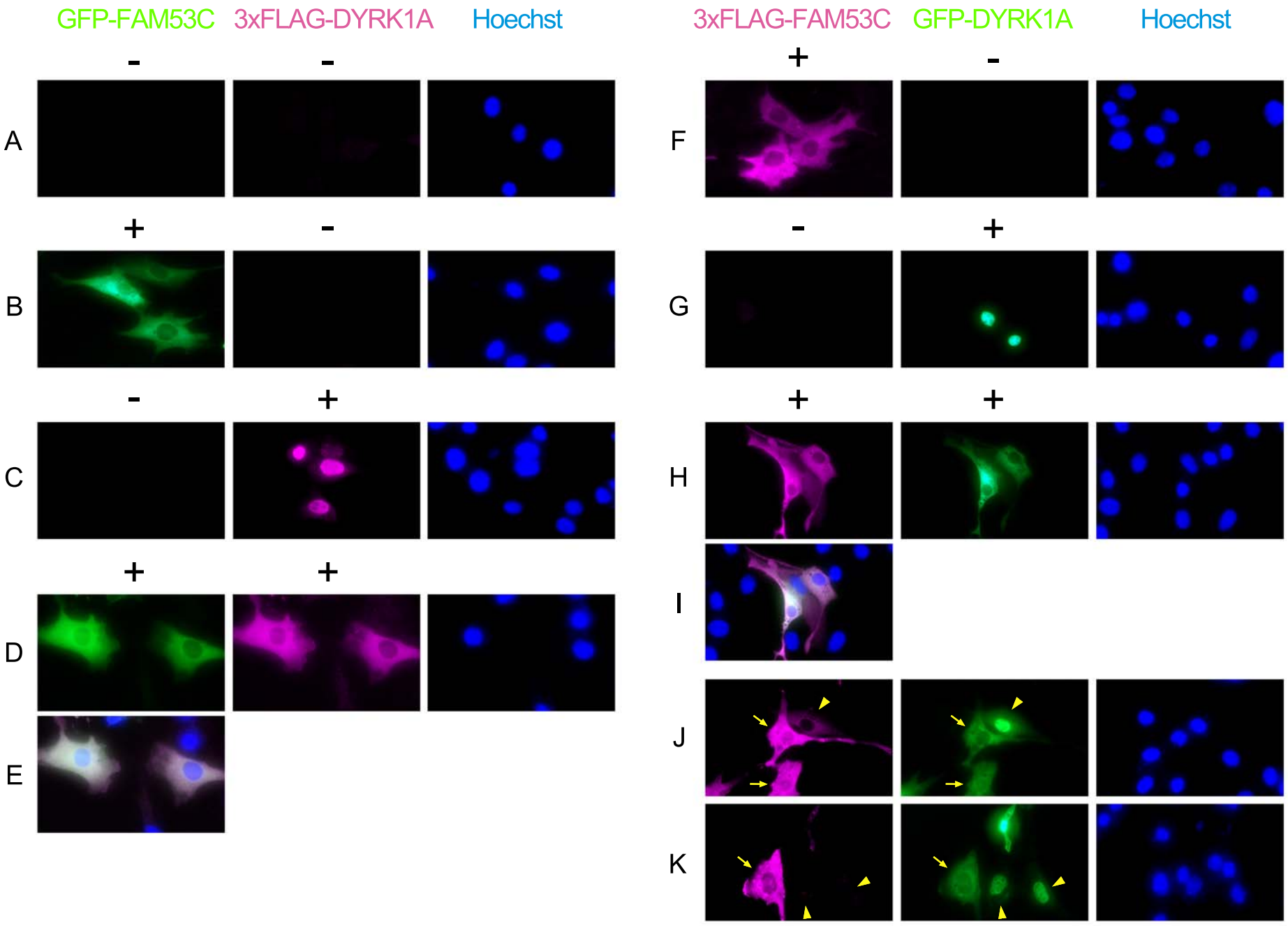
GFP-FAM53C
3xFLAG-DYRK1A
Hoechst
3xFLAG-FAM53C
GFP-DYRK1A
Hoechst
A
B
C
D
E
F
G
H
I
J
K

Figure 7

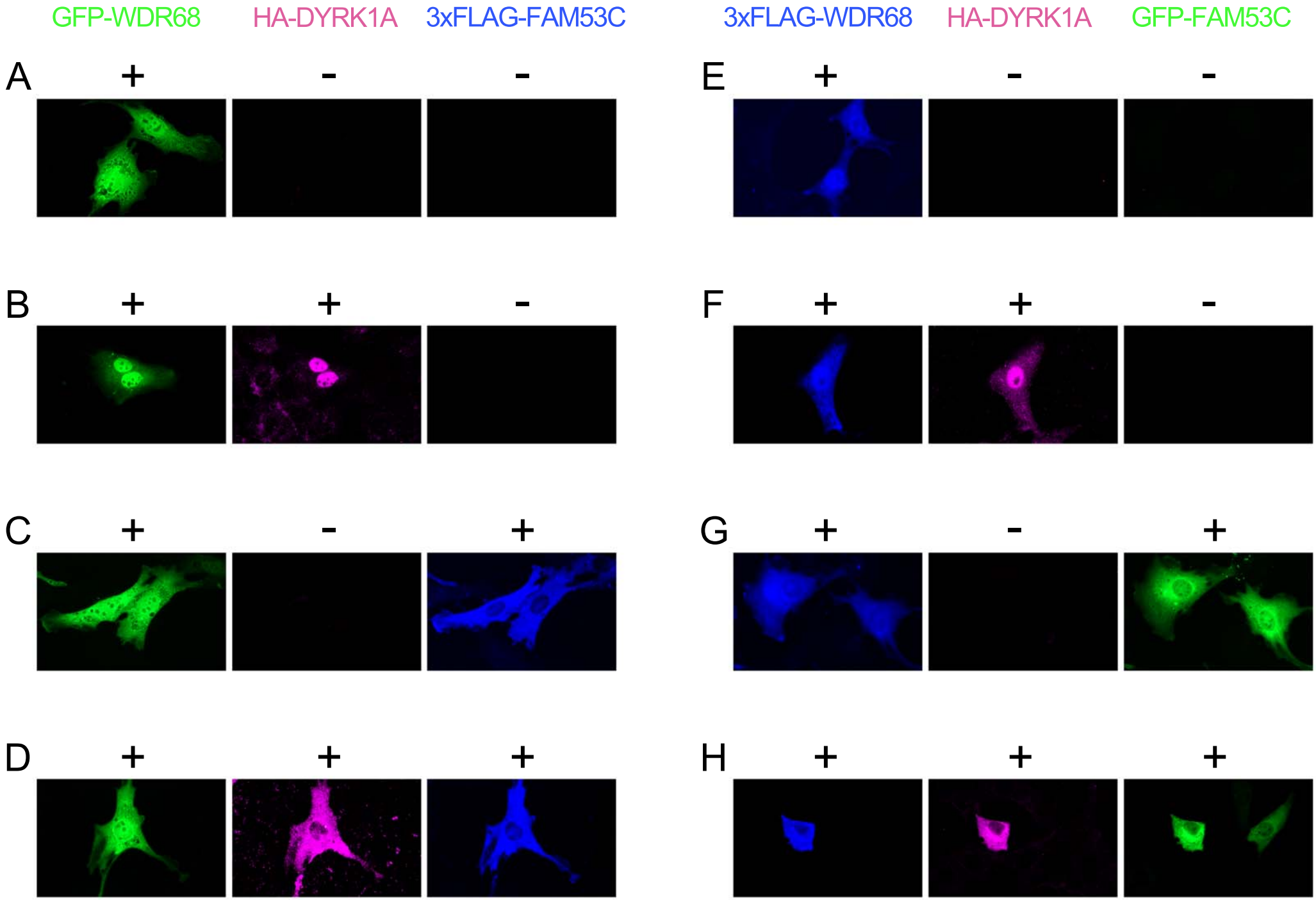
GFP-WDR68
HA-DYRK1A
3xFLAG-FAM53C
3xFLAG-WDR68
HA-DYRK1A
GFP-FAM53C
A + - -
B + + -
C + - +
D + + +
E + - -
F + + -
G + - +
H + + +

Figure 8

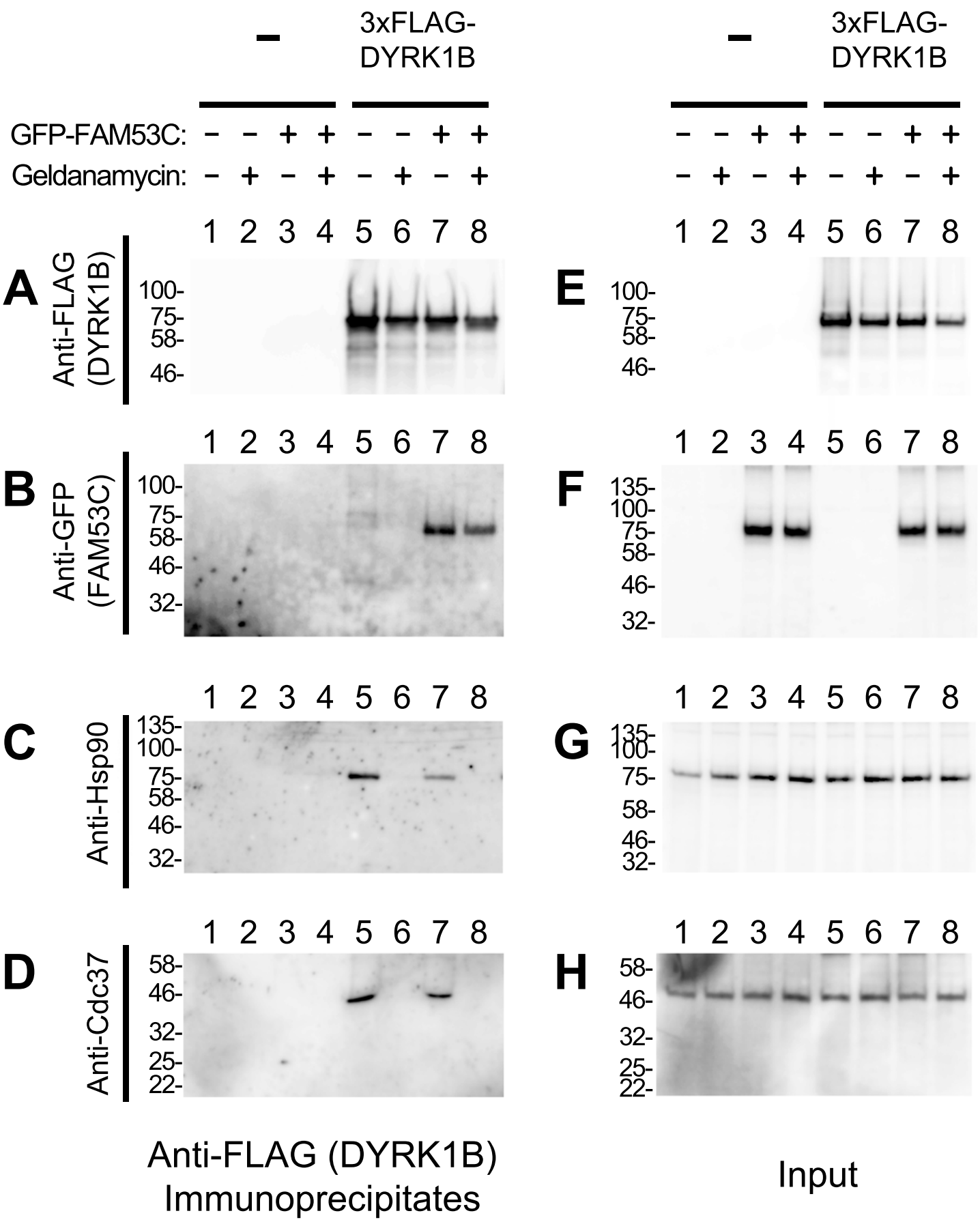
–
3xFLAG-DYRK1B
GFP-FAM53C: – – + + – – + +
Geldanamycin: – + – + – + – +
1 2 3 4 5 6 7 8
A
Anti-FLAG (DYRK1B)
100-
75-
58-
46-
B
Anti-GFP (FAM53C)
32-
C
Anti-Hsp90
135-
D
Anti-Cdc37
25-
22-
E
F
G
H
Anti-FLAG (DYRK1B) Immunoprecipitates
Input

Figure 9

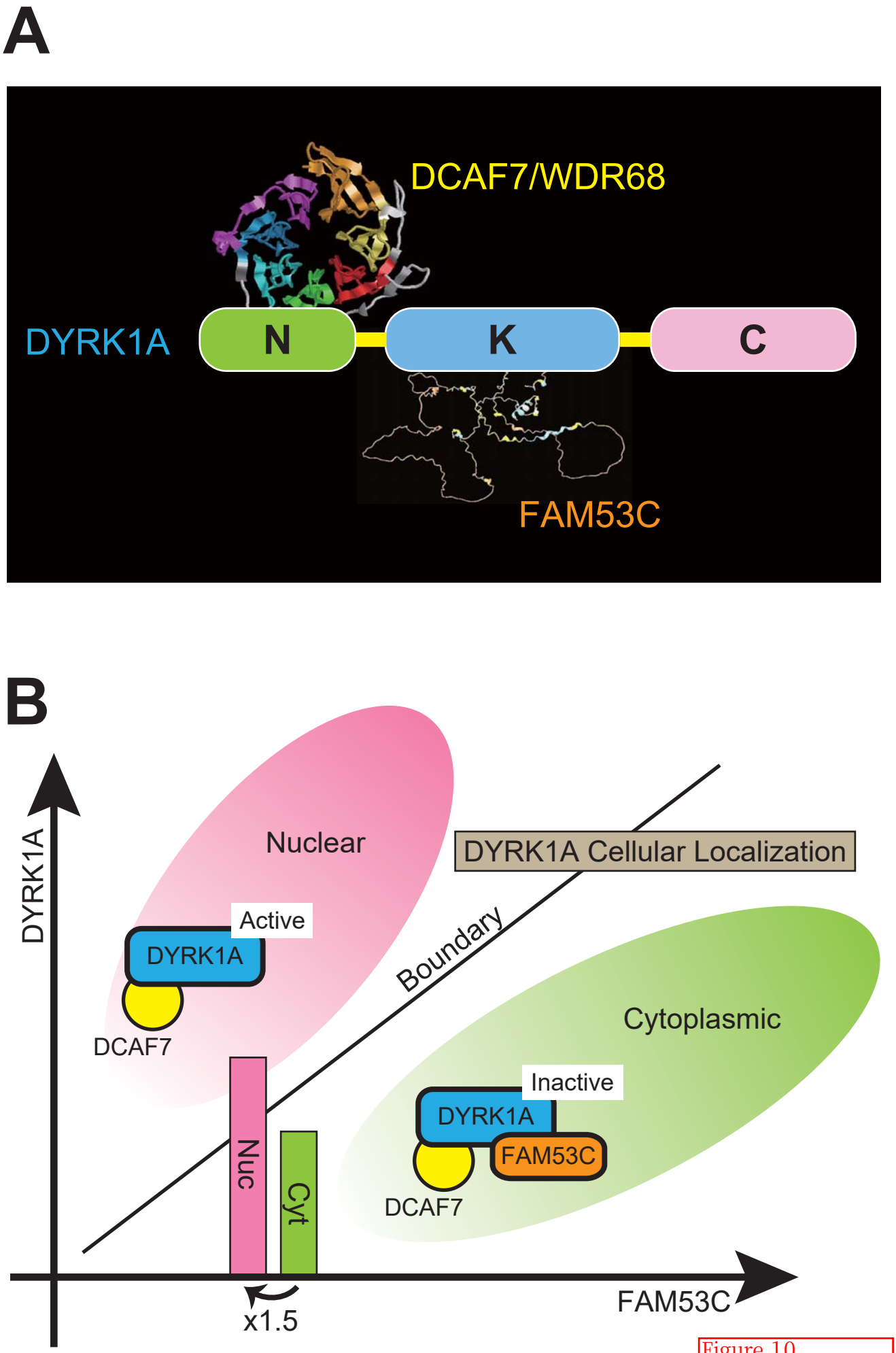
A
DCAF7/WDR68
DYRK1A
N
K
C
FAM53C
B
DYRK1A
Nuclear
DYRK1A Cellular Localization
Active
DYRK1A
DCAF7
Boundary
Cytoplasmic
Inactive
DYRK1A
FAM53C
DCAF7
Nuc
Cyt
x1.5
FAM53C

Figure 10